**Title**

Significance of *Naam* to Auditory Homeostasis and Auditory Circadian Rhythms in *Drosophila melanogaster*

**Course**

MRes Brain Sciences

**Module**

BRNF0003 Research Project

**Candidate Number**

SLZT6

**Word Count**

6599 (excl. references & appendix)

## Declaration

I confirm that the work presented in this thesis is my own. Where information has been derived from other sources, I confirm that this has been indicated in the thesis.


## Acknowledgements

This research was supported by Professor Jörg Albert's laboratory at the UCL Ear Institute.

## Personal Acknowledgements

My heartfelt gratitude goes to the infectiously enthusiastic Professor Jörg Albert for taking me under his wing and acquainting me with the lovely people at the Ear Institute. Amongst the loveliest are Modesta Blunskytė-Hendley, Ole Sudland, Chonglin Guan, Judy Bagi, and Alexandros Alampounti, to whom I am indebted for their help along the way.

## Abstract

As in many sensory systems, the auditory system of *Drosophila melanogaster* is gated by a circadian rhythm. The fly's antennal ear is an active sensor, injecting energy into sound-induced antennal motion. The antenna can be modelled as a moderately damped simple harmonic oscillator. The resonant frequency, frequency selectivity, and energy injection of this system vary over the circadian day. As in other sensory systems, this rhythm may be a signature of circadian homeostatic repair. This is likely mediated by a peripheral antennal molecular clock. However, the clock's homeostatic molecular control arms are poorly understood. *Naam*, encoding nicotinamidase, may play a regulatory role in circadian homeostasis downstream of the clock. We show that knockdown of *Naam* decreases the antenna's frequency selectivity and energy injection, and increases its resonant frequency. Additionally, *Naam* knockdown weakly interferes with the resonant frequency circadian rhythm. Our results are consistent with a role for *Naam* in auditory homeostasis. Further study is necessary to elucidate its precise role.


## Introduction

The fruit fly *Drosophila melanogaster* is a well-established model for the study of auditory neuroscience. *Drosophila*'s auditory system instantiates numerous organising principles conserved across the taxa. With reference to vertebrates, these similarities include biophysical mechanisms of auditory transduction[1] and amplification[2], the anatomical colocation of auditory and proprioceptive sensors and their afferent organisation[3], and molecularly conserved families of proneural genes coordinating auditory neurodevelopment. Notably, the *atonal* basic helix-loop-helix transcription factor[4] is functionally interchangeable with its vertebrate homologues (Math1/Atoh1 in mice and ATOH1 in man)[5 6].

Hearing in *Drosophila* is facilitated by the moderately damped simple harmonic oscillator represented by the pivot-joint-coupled second (a2) and third (a3) antennal segments. a3 is rigidly coupled to the arista (Figure 1a, b), jointly forming the sound receiver that converts the particle-velocity component of a sound wave into a sympathetic rotatory oscillation. This oscillation, via direct mechanical coupling, actuates mechanoreceptors inside a2 in a reciprocating manner[7] (Figure 1c). The ~500 a2 neurons, alongside their support cells, form Johnston's Organ (JO). JO neurons are divided into five subpopulations, with approximately half responding to vibratory stimuli such as sound, and half to more tonic stimuli such as wind and gravity[8]. The antennal receiver's resonant frequency increases continuously with stimulus intensity, revealing an intensity-dependent stiffness (Figure 1e). This is supplemented by an active process in which (probably Dynein[9]) motor proteins adjust the tension between the neurons' mechanosensitive ion channels and a3, thereby modifying the effective stimulus forces (Figure 1d). This non-linear frequency response sensitises *Drosophila* to near-field acoustic communication. This is critically important due to the reliance of fly mating on courtship songs[10].

As in many vertebrate auditory systems[11 12 13 14 15], the fly's auditory system may be gated by a circadian rhythm (n.b., ref.[16] unreviewed). Mechanosensory neurons vary the tension they apply to a3 with circadian time. This varies auditory sensitivity and amplification (indexed by *power gain*), consequently adjusting the resonant frequency (*best frequency*) and frequency selectivity (*tuning sharpness*) of the antennal oscillator throughout the day. As in many visual systems[17], this rhythm may be (partly or wholly) a signature of homeostatic repair. Circadian rhythms are established at a cellular level by the autonomous oscillations of molecular clock genes which regulate their own expression (Figure 1f). One such gene, *clk* (CLOCK), acts as a master regulatory transcription factor to temporally pattern cellular physiology and homeostasis[18].

Disrupting *clk* in the fly visual system disrupts *clk*-mediated gene regulatory networks resulting in impaired homeostasis and increased oxidative stress[19].

JO neurons possess molecular clocks[20] which presumptively pattern auditory homeostasis. Flies, like mammals, succumb to age-related hearing loss (ARHL), entering a phase of rapid terminal auditory decline during which the active energy injection process progressively fails. Analysis of JO's age-variable transcriptome implicates a battery of genes in ARHL. One of these genes, *Naam,* is significantly downregulated with age, and intersects four master-regulators associated with these age-related transcriptomic changes[21] (Figure 1g). *Naam* is among the most highly expressed JO genes (84$^{th}$ of 16,624)[22]. Additionally, *Naam* transcription in JO has been established to be under circadian modulation (Figure 1h).

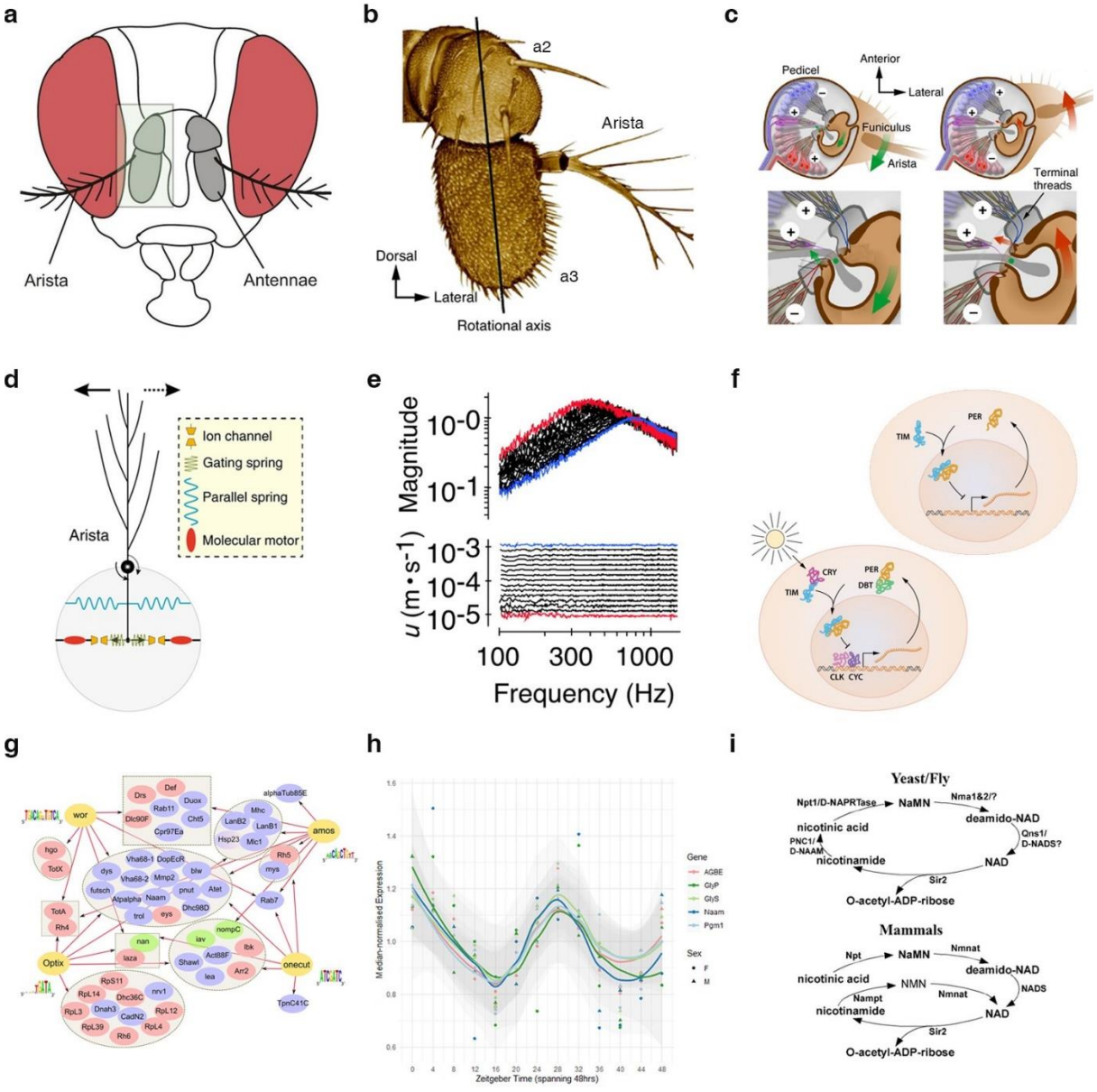


*Figure 1. a, b) Antennal anatomy (refs.[23, 24]). c) Transverse cross-section through a2 shows reciprocally actuated mechanoreceptors (ref.[24]). d) Within neuronal membranes, directly gated mechanotransducer channels associate with molecular motors to provide stimulus adaptation and amplification by adjusting tension on the arista (ref.[25]). e) Antennal response magnitudes (top) vary non-linearly vs. different stimulus particle velocities (bottom). Response magnitudes given as a ratio between vibration velocity and stimulus particle velocity (m·s−1/m·s−1) (ref.[26]). f) A simplified illustration of the molecular clock.* period *mRNA and PER oscillate, with PER oscillation lagging behind* period *mRNA. PER localizes in the nucleus, inhibiting its own transcription. Additional proteins refine this feedback*

*loop. TIM also oscillates and interacts with PER. This is critical for PER nuclear accumulation and repression of* period. *DBT is a protein kinase that phosphorylates PER, leading to its degradation. DBT-mediated PER degradation contributes to the lag between* period *mRNA and PER oscillation. CLK and CYK are two transcription factors that activate the period gene (ref.[27]). g) Prediction of upstream master regulators (yellow) for age-variable JO target genes with arrows leading to their predicted targets. Targets are grouped; up and down-regulated genes shown in blue and red respectively. Mechanosensory ion channels are shown in green (ref.[21]). h) Unpublished data: RNA sequencing of JO at 4-hour intervals (each data point is the mean of a biological triplicate of 280 JOs) in the circadian day across 48h reveals oscillatory concentrations of* Naam *RNA products, indicating circadian-regulated transcription of* Naam. AGBE, GlyP, GlyS, Pgm1, *and* Rpl32 *were identified as* Naam *protein-interaction partners using the STRING protein association network database[28]. The line shading envelope in this and all subsequent line plots denotes the standard error of the mean (SEM). i) NAD salvage pathways in yeast/flies and mammals;* Nampt *is the mammalian orthologue of* Naam (*ref.*[29]).

*Naam* encodes nicotinamidase, which catalyses the decomposition of nicotinamide into nicotinate and ammonia. Nicotinamidase is part of the salvage pathway of nicotinamide adenine dinucleotide (NAD+)[30] (Figure 1i). NAD+ is the central electron carrier in cellular metabolism, including respiration. NAD+ is also consumed in many non-redox processes such as ADP-ribosylation, cyclic-ADP-ribose production, and by NAD-dependent histone deacetylases (sirtuins: Sir2 homologues)[29]. Sirtuins are linked to cellular stress resistance and extended lifespan, regulating genes involved in mitochondrial function, apoptosis, inflammation, and many aspects of aging. *Naam*-overexpressing flies exhibit a Sir2-dependent increased mean lifespan of ~30%. Overexpression using *elavGal4* implicates neurons as the key mediator cell for *Naam*'s lifespan-extending effects[31]. Furthermore, sirtuins can rapidly deplete cellular NAD+, resulting in increased concentrations of nicotinamide, which acts as a potent sirtuin inhibitor. Therefore, NAAM is critical to the salvage pathway that both replenishes NAD+ and reduces nicotinamide negative feedback[29]. Additionally, fluctuations in the NAD+/NADH (the reduced form of NAD+) ratio, a function of satiety, can entrain the molecular circadian clock[32 33].

The NAD+/NADH ratio is an index of cellular reduction potential and is regulated by small changes in NAD+ concentration. NAD+/NADH ratio shifts towards NADH are pro-senescent; NADH competitively inhibits sirtuins and facilitates reactive oxygen species (ROS) formation[30]. ROS are generated by mitochondria during cellular respiration and are normally cleared by antioxidant scavengers. Protective antioxidant mechanisms degenerate with age, leading to ROS overproduction and subsequent oxidative stress[34]. *Naam* confers resistance to oxidative stress. PNC-1 (a *Naam* homologue) overexpression increased lifespan in *C. elegans* under conditions of oxidative stress[35], and flies responding to oxidative stress show a six-fold increase in *Naam* mRNA transcription and translation[29]. Oxidative stress is implicated in mammalian cochlear senescence due to the cochlea's high metabolic rate[36], and may likewise underlie ARHL in *Drosophila.* This would accord with the downregulation of *Naam* in JO contemporaneous with ARHL[21].

The *Drosophila* evidence for *Naam* function comes from non-auditory-specific overexpression studies and does not directly address whether *Naam* is part of a normal homeostatic mechanism. Nevertheless, there is enough evidence to indicate that manipulating *Naam* may disrupt the putative circadian patterning of homeostatic repair, potentially influencing circadian auditory rhythms. Therefore, we hypothesise **primarily** that JO-targeted *Naam* knockdown will alter the auditory circadian rhythm, and **secondarily**, overall auditory function.

# Methods

## Fly Lines

We used the TARGET system[37], in which ubiquitously-expressed temperature-sensitive Gal80 ($Gal80^{ts}$) inhibits Gal4 (a yeast transcriptional activator) at low (permissive) temperatures, but

inactivates at 29–30°C (restrictive temperature), allowing Gal4 to bind to its DNA binding motif, upstream activating sequence (UAS). To silence *Naam* transcription, we used an NP0761-Gal4 driver line[38] to drive JON-restricted expression of a UAS-hairpin *Naam* RNAi (RNA interference) construct integrated at the attP40 docking site[39] (Figure 2a). Crossing the driver line with an 'empty' attP40 cassette line yielded a control line with a similar genetic background. Crossing the driver line with an attP40-integrated UAS-EGFP-containing P-element line yielded our reporter.

Maternal flies of the genotype yw; tub-Gal80/tub-Gal80; NP0761/TM6B were crossed with y[1] sc[*] v[1] sev[21]; P{y[+t7.7] v[+t1.8]=TRiP.HMS02770}attP40, y[1] v[1]; P{y[+t7.7]=CaryP}attP40, and w[1118]; P{w[+mC]=UAS-EGFP}5a.2 fathers (paternal lines were obtained from the Bloomington *Drosophila* Stock Centre). These crosses respectively produced the genotypes ;; tub-Gal80/ P{y[+t7.7] v[+t1.8]=TRiP.HMS02770}attP40; NP0761/+ (*Naam* RNAi flies), ;; tub-Gal80/ P{y[+t7.7]=CaryP}attP40; NP0761/+ (attP40 control flies), and ;; tub-Gal80/ P{w[+mC]=UAS-EGFP}5a.2; NP0761/+ (reporter flies).

## Rearing Conditions

Flies were raised on standard medium (changed twice weekly) in environmentally controlled incubators (130VL, Percival Scientific, USA) maintained at 25°C and 70% relative humidity (RH), with a 12:12h light:dark entrainment regime. Male flies were used for all experiments. *Naam* RNAi knockdown mutants were kept at 18°C in their larval and pupal stages to repress Gal4-mediated transcriptional activation by a $Gal80^{ts}$ repressor. Mutants were collected on the day of eclosion and transferred to 30°C for adult-specific activation of the Gal4/UAS transcription system.

## Sample Preparation & Confocal Fluorescence Microscopy

Fly heads of 12-day-old flies raised at 25°C and 30°C were detached and immersed in acetone to permeabilise the cuticle, then washed with 70% ethanol and type I ultrapure water. Samples were mounted onto slides while suspended in an anti-fading agent (1,4-diazabicyclo[2.2.2]octane (DABCO)). Images were acquired using the GFP fluorescence channel (excitation wavelength: 488nm; emission bandwidth 464-633nm) of a LSM 510 Zeiss confocal microscope with a Plan-Apochromat 20×/0.80 M27 dry objective. Z-stacks (optical slice thickness: 1µm, 25 slices in total) were taken throughout JO. ImageJ (Fiji) was used for image analysis and assembly.

## Behavioural Experiments

Circadian locomotor rhythms were assessed by placing $CO_2$-aneasthetised one-day-old male flies into glass tubes containing a 4% sucrose, 2% agar medium fly food, which were housed in *Drosophila* Activity Monitors (DAM-5M, TriKinetics, USA). Monitors were placed in an incubator maintained at 30°C and 70% RH, running a 12:12h LD entrainment programme. The experiment lasted three days, from days 2-4 of age. The DAM-5M system records infrared beam (four per tube) breaks of flies walking in the glass tubes at one minute time-resolution as an activity index (Figure 2d, e).

We generated an artificial 'song' controlled using Spike2 software (Cambridge Electronic Design Ltd., England). A single artificial pulse was composed by averaging ~1000 pulses from mating songs recorded within a sound chamber from 10 flies. A 2s artificial pulse train composed of artificial pulses separated by 40ms inter-pulse intervals followed by a 2s silence period (Figure 2f) was played continuously for fifteen minutes, followed by forty-five minutes of silence. This sequence was looped hourly across the 24h day.

This song was introduced via a custom-built vibration platform allowing the stimulus to present both acoustically and as a substrate-borne vibration. The Spike2 sequence was outputted via a linear power amplifier (LDS-LPA100) to a permanent magnet shaker (V201-M4-CE) which actuated an acrylic mounting platform (all Brüel & Kjær, Denmark). DAM-5M monitors were affixed to the platform using 3D-printed mounts. Data were recorded using the TriKinetics DAMSystem3 data acquisition software.

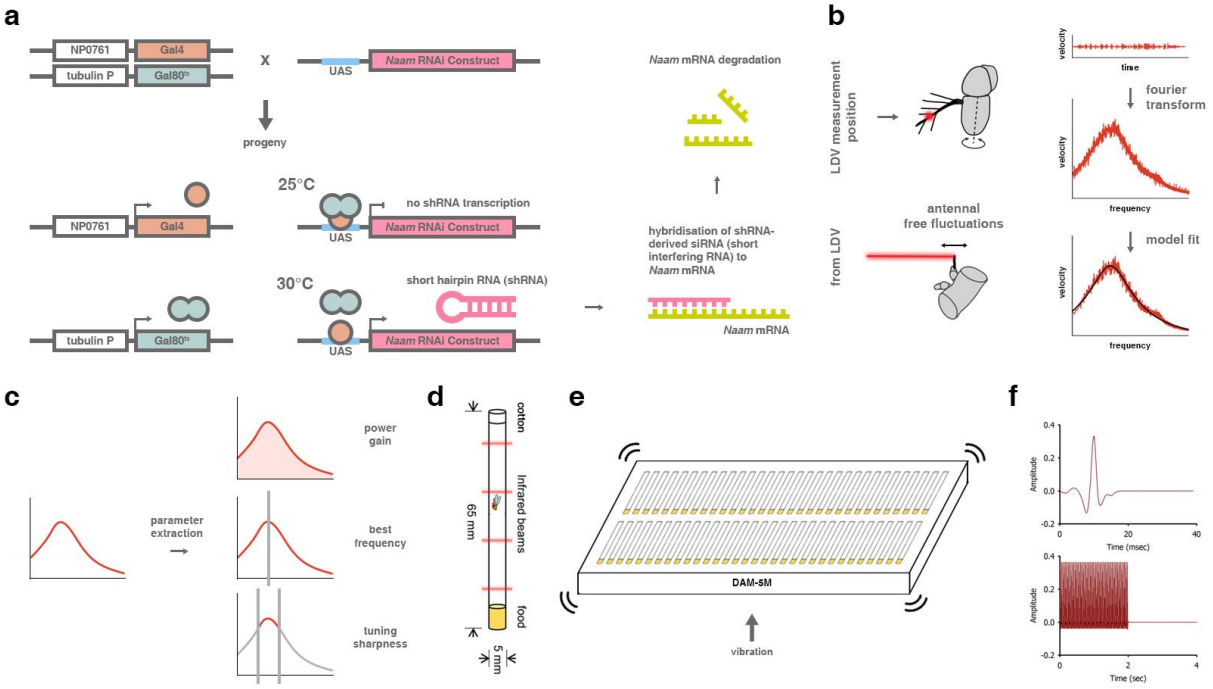


*Figure 2: Graphical overview of methods (descriptions in methods).*

## Antennal Measurements

The measurement procedure accords with an established protocol[1 40]. *Naam* RNAi and attP40 control flies were raised together from eclosion at 25 °C or 30 °C in equal numbers for the respective temperature experiment arms. Half of the flies were aged for 12d and half for 13d. Across all four groups, 30 flies were measured twice (60 measurements) for each of four timepoints in the 24-hour day (zeitgeber time 0 (ZT0, 'lights on'), ZT6, ZT12, and ZT18). Thus, ~960 measurements were taken of ~480 flies.

Flies were cooled to induce a chill-coma. They were then fixated ventrum-down to the head of a Teflon rod using a blue-light cured dental adhesive, ensuring stabilisation of their heads, wings, legs, and halteres (spiracles were unobstructed). The second segment of the antenna was fixated to prevent non-auditory background displacements. The contralateral antenna was immobilised to abolish any interference with the recordings. After mounting, flies recovered for at least fifteen minutes before orientation to align the arista perpendicular to a laser doppler vibrometer (LDV) beam at a focal distance of 70mm (Figure 2b). Mounting occurred under red light (and LDV recordings in darkness) so as not to reset the animals' circadian clocks.

The LDV (PSV-400, Polytec, Germany) was equipped with an OFV-70 close-up unit and a DD-5000 displacement decoder. The laser was focused on the arista tip with the laser head's scanning unit. Laser-spot position (diameter ~5µm) was continuously monitored via an integrated coaxial video-capture system. Simultaneously, a grounding electrode was placed against the thorax to prevent static interference. Recordings were made between 18 °C–21 °C. An active vibration isolation table (63-564; TMC, USA) was used. Mutant and control animals were recorded in

alternating fashion to evenly distribute random systemic variation. Each recording was made for 60s at a sampling rate of 8,192Hz.

## Data Analysis

### Antennal Measurements

Recordings of velocity with respect to time were Fast-Fourier-transformed (60 averaged time windows, rectangular windowing function, 1000ms window length) at 1Hz resolution from 50-3200Hz using PSV Software. Non-linear least squares analysis was used to fit a simple harmonic oscillator model (discussed in ref.[40]) to the Fast-Fourier-transformed data following outlier removal in R. This produced a Cauchy–Lorentz frequency distribution for each recording (Figure 4a) – effectively an antennal tuning curve[41] – from which indexes of auditory system function could be extracted. Best frequency corresponds to the frequency at the maximum of this distribution and describes the receiver's natural frequency. Tuning sharpness corresponds to the resonance frequency range (i.e., frequency selectivity) and is proportional to the distribution's kurtosis. Power gain corresponds to the amount of energy injected (by gating-spring motors in JO neurons) into the system and is related to the area under the distribution curve (Figure 2b, c; further discussion may be found in ref.[2]).

These three parameters were extracted from each distribution for statistical analysis and grouped by level across all three independent variables. As the data were non-parametric, an aligned rank transformation (ART)[42] was conducted before performing factorial (two- and three-way) ANOVAs and ART-based (Holm-Sidak) contrast tests[43]. These were facilitated by the ARTool[44] package for R.

### Behavioural Experiments

DAM-5M recordings were exported from the DAMSystem3 Software for analysis in R. The Rethomics package[45] was used for high-throughput behavioural analysis. Data were non-parametric; two-way repeated measures ART ANOVAs were conducted with ART-based (Holm-Sidak) contrast tests.

# Results

To interrogate the functional importance of *Naam* to the performance and circadian rhythms of the auditory system, we used a JO-neuron-specific Gal4 driver line in combination with a temperature-sensitive transcriptional inhibitor of Gal4 ($Gal80^{ts}$) and a UAS-RNAi *Naam* knockdown construct (see methods). Silencing of *Naam* was initiated by transferring flies to a 30°C environment post-eclosion to exclude neurodevelopmental confounds. Transcription efficacy was validated by crossing our driver line with a UAS-EGFP (enhanced green fluorescent protein) responder line (Figure 3). We crossed the driver line with an 'empty' attP40 cassette line to obtain a control line with a similar genetic background.

*Naam* RNAi and attP40 control flies were subjected to a battery of assays: genetic, then biomechanical, and finally behavioural. Firstly, RT-qPCR assays were conducted to (1) verify if *Naam* expression in the flies' bodies is rhythmic, and (2) confirm *Naam*-knockdown in the RNAi animals. These results have been provided in the appendix as we were unable to meet the MIQE guidelines[46] for minimum biological replicate number ($n \geq 3$). Secondly, laser-doppler vibrometry was used to interrogate differences in antennal mechanics across genotypes, temperatures, and circadian timepoints. Finally, activity monitors were used to investigate genotypic differences in circadian rhythms and responses to ethologically salient sounds.

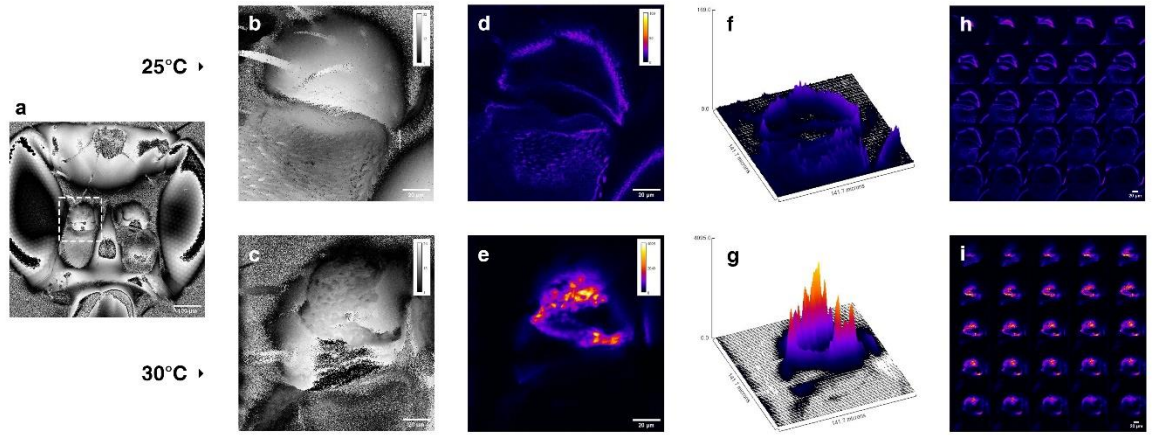


*Figure 3: Validation of the temperature-dependent JO-neuron-specific transcription activation system. Top and bottom rows show images from 12-day-old reporter flies raised at 25 °C and 30 °C respectively, imaged under the same settings. a) Topography map of a z-stack of the head of a reporter fly, showing the location of subsequent images. b, c) Topography maps showing the locations of a2 and a3; legends refer to z-stack slice. d, e) Intermediate z-stack slice clearly showing higher Gal4-driven expression of EGFP at 30 °C vs 25 °C in JO neurons; legends show colour look-up table. f, g) Surface plots of fluorescence intensity, note scaled z-axes. h, i) Montages of z-stacks through JO in the anteroposterior axis; some cuticular autofluorescence is seen in the anterior a2 (top rows).*

## Antennal Free Fluctuations Reveal Marked Phenotypic Differences

Antennal free fluctuations (responses of unstimulated antennae to the air's Brownian motion) of *Naam* RNAi and attP40 control flies were measured across four timepoints (ZT0, ZT6, ZT12, and ZT18) and two rearing temperatures (25 °C and 30 °C) on days 12 and 13 of a 12:12h LD entrainment regime. Non-parametrised two- and three-way ANOVAs were performed to analyse the effects of genotype, zeitgeber time, and temperature on power gain, best frequency, and tuning sharpness. Within-genotype and within-temperature-group two-way ANOVAs are presented in the appendix, alongside all contrast estimates and respective standard errors, t-ratios, and p-values.

With respect to power gain, there exists no statistically significant interaction between the effects of temperature, genotype and zeitgeber time. Additionally, no pair of these factors interacted significantly. However, each factor was independently significant. Three-way ANOVA results for simple main effects and factorial interactions are shown in Table 1.

*Table 1: 3-way ANOVA results with respect to power gain.*

| Factor(s) | Degrees of Freedom | Residual Degrees of Freedom | F-value | p-value |
|---|---|---|---|---|
| Temperature | 1 | 946 | 44.188 | 5.03E-11 |
| Genotype | 1 | | 245.855 | 1.98E-49 |
| Zeitgeber Time | 3 | | 6.232 | 3.43E-4 |
| Temperature * Genotype | 1 | | 1.425 | 0.232 |
| Temperature * Zeitgeber Time | 3 | | 0.652 | 0.581 |
| Genotype * Zeitgeber Time | 3 | | 1.129 | 0.336 |
| Temperature * Genotype * Zeitgeber Time | 3 | | 0.148 | 0.931 |

With respect to best frequency, there exists no statistically significant interaction between the effects of temperature, genotype and zeitgeber time. Additionally, temperature interacted

significantly with genotype and zeitgeber time, and each factor was independently significant. Three-way ANOVA results for simple main effects and factorial interactions are shown in Table 2.

*Table 2: 3-way ANOVA results with respect to best frequency.*

| Factor(s) | Degrees of Freedom | Residual Degrees of Freedom | F-value | p-value |
|---|---|---|---|---|
| Temperature | 1 | 946 | 338.791 | 6.62E-65 |
| Genotype | 1 | | 98.573 | 3.64E-22 |
| Zeitgeber Time | 3 | | 2.714 | 0.0438 |
| Temperature * Genotype | 1 | | 19.253 | 1.27E-05 |
| Temperature * Zeitgeber Time | 3 | | 13.957 | 6.56E-09 |
| Genotype * Zeitgeber Time | 3 | | 1.675 | 0.171 |
| Temperature * Genotype * Zeitgeber Time | 3 | | 1.617 | 0.184 |

With respect to tuning sharpness, there exists no statistically significant interaction between the effects of temperature, genotype and zeitgeber time. The only significant 2-way interaction was between temperature and genotype. These two factors were the only two which were independently significant. Three-way ANOVA results for simple main effects and factorial interactions are shown in Table 3.

*Table 3: 3-way ANOVA results with respect to tuning sharpness.*

| Factor(s) | Degrees of Freedom | Residual Degrees of Freedom | F-value | p-value |
|---|---|---|---|---|
| Temperature | 1 | 946 | 105.821 | 1.34E-23 |
| Genotype | 1 | | 23.246 | 1.66E-06 |
| Zeitgeber Time | 3 | | 1.612 | 0.185 |
| Temperature * Genotype | 1 | | 24.213 | 1.02E-06 |
| Temperature * Zeitgeber Time | 3 | | 0.941 | 0.420 |
| Genotype * Zeitgeber Time | 3 | | 0.776 | 0.508 |
| Temperature * Genotype * Zeitgeber Time | 3 | | 1.034 | 0.377 |

For all ANOVAs, post-hoc analysis was carried out using the Holm-Sidak method (pairwise contrast estimates are visualised in Figure 4c). All 120 contrast estimates and respective standard errors, t-ratios, and p-values are provided in the appendix.

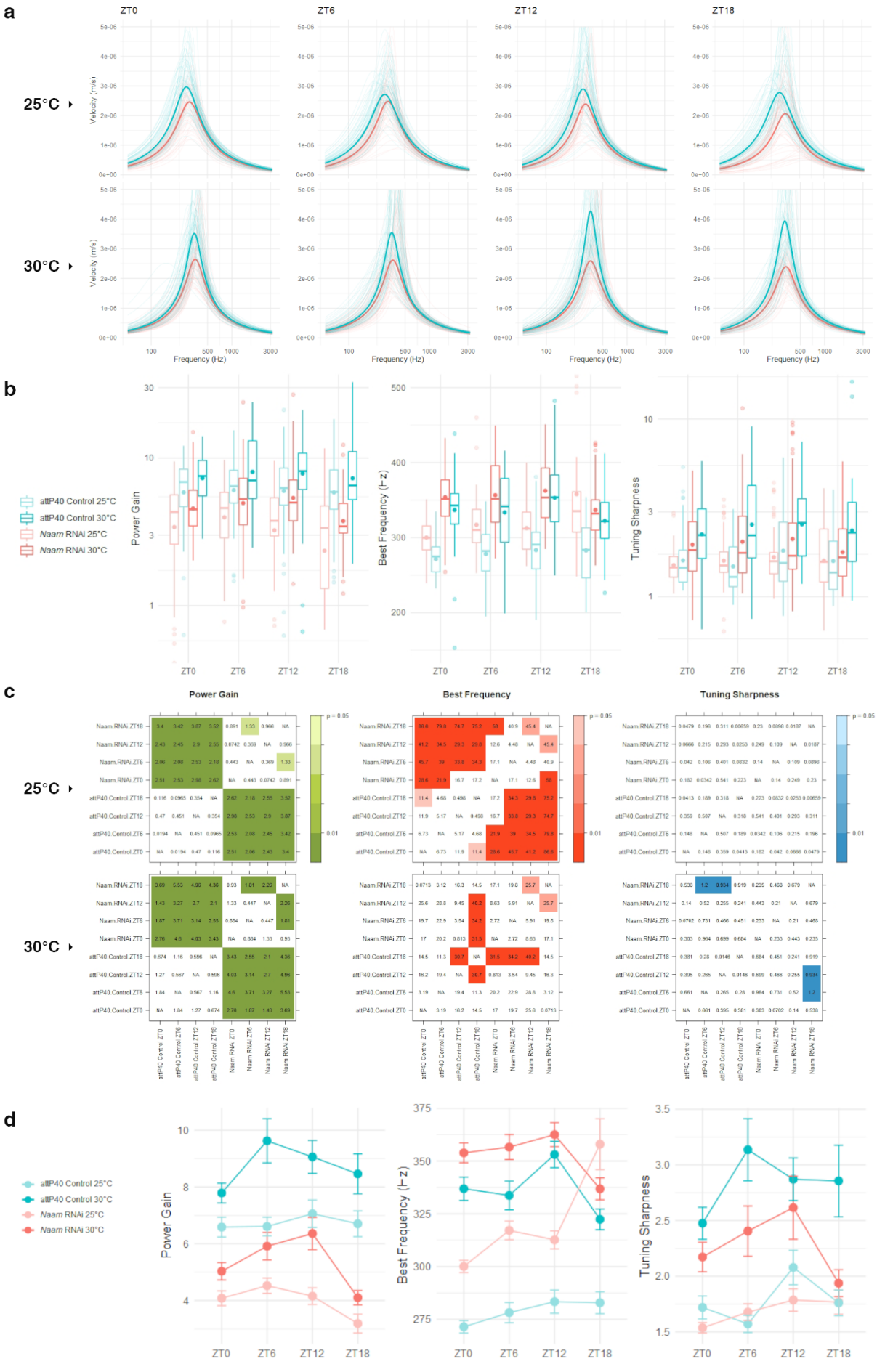
a
ZT0
ZT6
ZT12
ZT18
25°C
30°C
Velocity (m/s)
Frequency (Hz)
b
attP40 Control 25°C
attP40 Control 30°C
Naam RNAi 25°C
Naam RNAi 30°C
Power Gain
Best Frequency (Hz)
Tuning Sharpness
c
Power Gain
Best Frequency
Tuning Sharpness
d
Power Gain
Best Frequency (Hz)
Tuning Sharpness

*Figure 4: a) Simple harmonic oscillator model fits to fast-fourier-transformed recordings of antennal velocity vs. time, grouped by timepoint and rearing temperature. Colour conventions are analogous to box plot conventions (red lines represent mutants, blue lines represent controls). Thin lines correspond to individual measurements (for all groups, n=60±3); thick lines to the median. For each distribution, area under the curve is related to power gain, the maximum corresponds to best frequency, and kurtosis is proportional to tuning sharpness. The box plots (b) visualise these extracted values. Note the logarithmic frequency axes.*

*b) Box plots for all zeitgeber timepoints colour-coded by genotype and temperature, in the style of Tukey (opaque dot corresponds to the mean, thick horizontal line corresponds to the median, lower and upper hinges correspond to the first and third quartiles, whiskers extend to values up to 1.5 times the interquartile range from the hinges, and translucent points show outliers beyond this range). Power gain and tuning sharpness are dimensionless and are plotted logarithmically. Some outliers are not shown.*

*c) Holm-Sidak-corrected pairwise comparison matrices of means for power gain, best frequency, and tuning sharpness for all four zeitgeber timepoints within and across genotype, colour-coded by p-value. Magnitudes only are shown; direction can be obtained by comparison with line plots (d). The matrices can be split into quadrants such that the top-left and bottom-right quadrants compare across genotypes, whilst top-right and bottom-left quadrants compare within genotypes (i.e. showing only within-genotype circadian fluctuations). Pairwise comparisons across all three factors are not presented due to quantity and as individual timepoint-comparisons across temperatures are irrelevant – only circadian pattern differences across temperatures are of direct interest. The respective 120 pairwise comparisons are presented in the appendix.*

*d) Line plots displaying means for each genotype/temperature group across the three parameters of interest. Error bars show SEMs.*

Power gain exhibited no circadian rhythm (defined as a significant difference in the parameter of interest across timepoints) in attP40 controls raised at either temperature. Contrastingly, the mutant flies exhibit significant circadian variation in power gain at both temperatures. In mutants raised at 25°C, power gain maximised at ZT6 (mean=4.5) and minimised at ZT18 (mean=3.2, difference=1.3, p=0.036). In mutants raised at 30°C, power gain shifted its maximum later to ZT12 (mean=6.4) and continued to minimise at ZT18 (mean=4.1, difference=2.3, p=9.36e-4), with the amplitude of circadian modulation increasing. Whilst this may appear significant, the ANOVA reports that this interaction of genotype with zeitgeber time is non-significant (Table 1, F(3, 946)=1.129, p=0.336) with respect to effect on power gain.

Best frequency demonstrated circadian rhythmicity in both genotypes at both rearing temperatures. In the attP40 flies raised at 25°C, best frequency maximised at ZT18[a] (mean=282Hz) and minimised at ZT0 (mean=271Hz, difference=11Hz, p=0.046). When these flies were raised at 30°C, this pattern was shifted earlier in the day; best frequency maximised at ZT12 (mean=353Hz) and minimised at ZT18 (mean=322Hz, difference=31Hz, p=3.90e-3). In the mutant flies raised at 25°C, best frequency maximised at ZT18 (mean=358Hz) and minimised at ZT0 (mean=300Hz, difference=58Hz, p=6.80e-5). When raised at 30°C, this pattern was shifted earlier in the day; best frequency maximised at ZT12 (mean=363Hz) and minimised at ZT18 (337Hz, difference=26Hz, p=0.037). Notably, the mutant versus control difference of differences (i.e., across-genotype differences of within-genotype best frequency maximum-minimum ranges) is much higher at the rearing temperature of 25°C (47Hz) than 30°C (5Hz). The ANOVA reports that this interaction of genotype with zeitgeber time is not significant (Table 2, F(3, 946=1.675, p=0.171) with respect to effect on best frequency. However, it appears that increasing rearing temperature counteracts the effects of *Naam* knockdown (despite the presumed increased expression of the knockdown construct). This is supported by the two-way ANOVAs conducted within temperature groups (see appendix), which reported a significant interaction between genotype and zeitgeber time at 25°C but not 30°C (respectively, (F(3, 470)=2.945, p=0.0326; F(3, 476)=0.252, p=0.860) with respect to effect on best frequency.

[a] Best Frequency in fact maximised at ZT12 (283Hz), but this was non-significant (p=0.054) against ZT0.

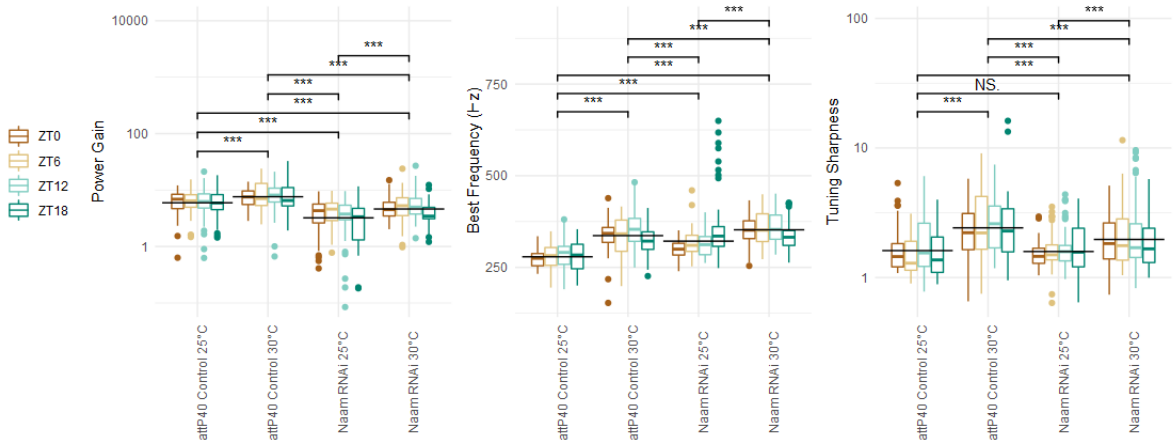


*Figure 5: Holm-Sidak-adjusted pairwise comparisons across temperatures and genotypes for power gain, best frequency, and tuning sharpness show the ZT-agnostic overall impact of temperature and genotype on the three parameters of interest. Respective means (black horizontal bars), from left to right: power gain (0.774, 0.882, 0.507, 0.664), best frequency (279Hz, 337Hz, 321Hz, 352Hz), and tuning sharpness (0.208, 0.383, 0.201, 0.294). For this and all subsequent figures, 'NS', p>0.05; '*', p≤0.05, '**', p≤0.01, '***', p≤0.001.*

Finally, a two-way ANOVA was conducted within the genetic control group (see appendix) to establish the significance of the aforementioned interaction of temperature with zeitgeber time (i.e., the genotype-agnostic best frequency rhythm phase-shift) without the confound of temperature-dependent knockdown in the mutant group. This best frequency phase-shift is indeed significant ($F(3, 475)=3.770$, $p=0.0107$) independently of *Naam* knockdown.

Tuning sharpness displayed no circadian rhythm in either genotype raised at either temperature. This is consistent with the ANOVA findings for the interaction between genotype and zeitgeber time (Table 3, $F(3, 946)=0.776$, $p=0.508$) with respect to effect on tuning sharpness.

Circadian interactions aside, JO *Naam* knockdown mediates an overall decrement in auditory performance (decreasing power gain (mean difference=0.19, p=1.98e-49) and tuning sharpness (mean difference=0.10, p=1.66e-06), and increasing best frequency (mean difference=29Hz, p=3.64e-22), moving it away from the ethologically salient 160-210Hz range[47] (Figure 5 and appendix)). This reciprocal movement is consistent with the understanding that decreased power gain in the antennal amplifier increases best frequency and decreases tuning sharpness[24].

## Knockdown Animals Exhibit a Distinct Behavioural Phenotype

We then investigated whether attenuated auditory sensitivity would translate to altered circadian locomotor rhythms and behavioural responses to sound. Mutants and controls were entrained to a 30°C 12:12h LD cycle from eclosion, with continuous minute-resolution activity monitoring for three days (spanning days 2-4 of the flies' age). On the third day, an artificial mating-song-derived stimulus was played for fifteen minutes at hourly intervals via a vibrating platform to assess both genotypes' sound responses.

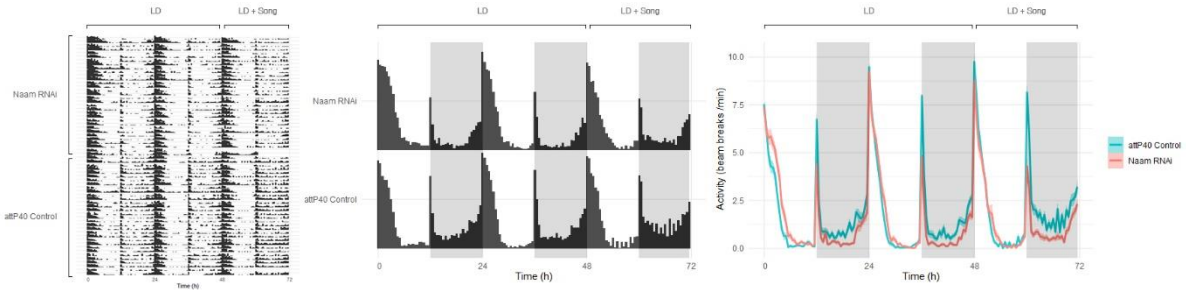


*Figure 6: Overall strategy (LD corresponds to experimental days 1-2; LD+Song corresponds to experimental day 3). Left panel: activity plots for individual* Naam *RNAi (n=32) and attP40 control (n=32) flies. The middle panel shows mean activity levels for each group. These plots are superimposed in the rightmost panel. Grey overlays indicate virtual 'night'. All data are plotted in thirty-minute bins. Clear morning and evening anticipatory peaks manifest, mediated by the circadian clock. This is typical of* Drosophila *in a rectangular LD cycle at constant temperature[48].*

## Mutant Flies Exhibit Altered Circadian Rhythms

A non-parametrised repeated-measures two-way ANOVA of activity during the LD phase of the experiment revealed a statistically significant interaction between the effects of genotype and zeitgeber day/night ($F(1, 184477)=71.558$, $p<2.22e-16$). Simple main effects analysis showed that both genotype ($F(1, 184477)=484.790$, $p<2.22e-16$) and zeitgeber day/night ($F(1, 184477)=1465.768$, $p<2.22e-16$) have a statistically significant effect on activity.

Post-hoc analysis using the Holm-Sidak correction found all pairwise comparisons significant at the $p<0.001$ level, visualised in Figure 7.

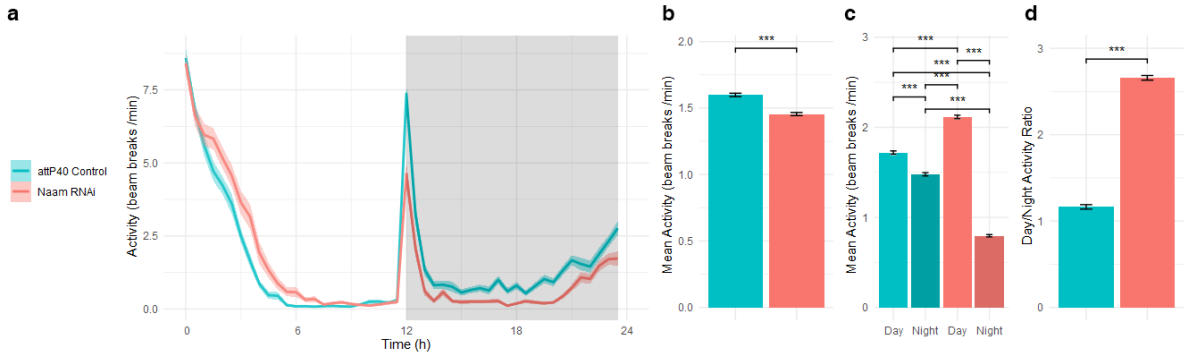


*Figure 7: Activity comparisons for the LD phase. a) The 'average day': line plots of mean genotype activity with respect to ZT at half-hour time resolution, averaged over both LD days. b) Mean genotype activity across both days; mutants show significantly lower activity (mean difference=0.11 beam breaks/min, p<2.22e-16). Error bars show the SEM. c) Holm-Sidak-computed pairwise comparisons across genotypes and day/night; all are significant at the p≤0.001 level. d) Genotype day/night activity ratios; mutants exhibit a highly significant daylight preference relative to the controls (ratio difference=1.49, p<2.22e-16).*

## Mutant Flies Show Altered Locomotor Responses to Song Stimulus

A non-parametrised repeated-measures two-way ANOVA of activity during the LD+Song phase of the experiment revealed a statistically significant interaction between the effects of genotype and song/silence ($F(1, 92125)=42.043$, $p<8.98e-11$). Simple main effects analysis showed that both genotype ($F(1, 92125)=3772.078$, $p<2.22e-16$) and song/silence ($F(1, 92125)=145.425$, $p<2.22e-16$) have a statistically significant effect on activity.

Post-hoc analysis using the Holm-Sidak correction found all pairwise comparisons significant at the p<0.001 level, visualised in Figure 8.

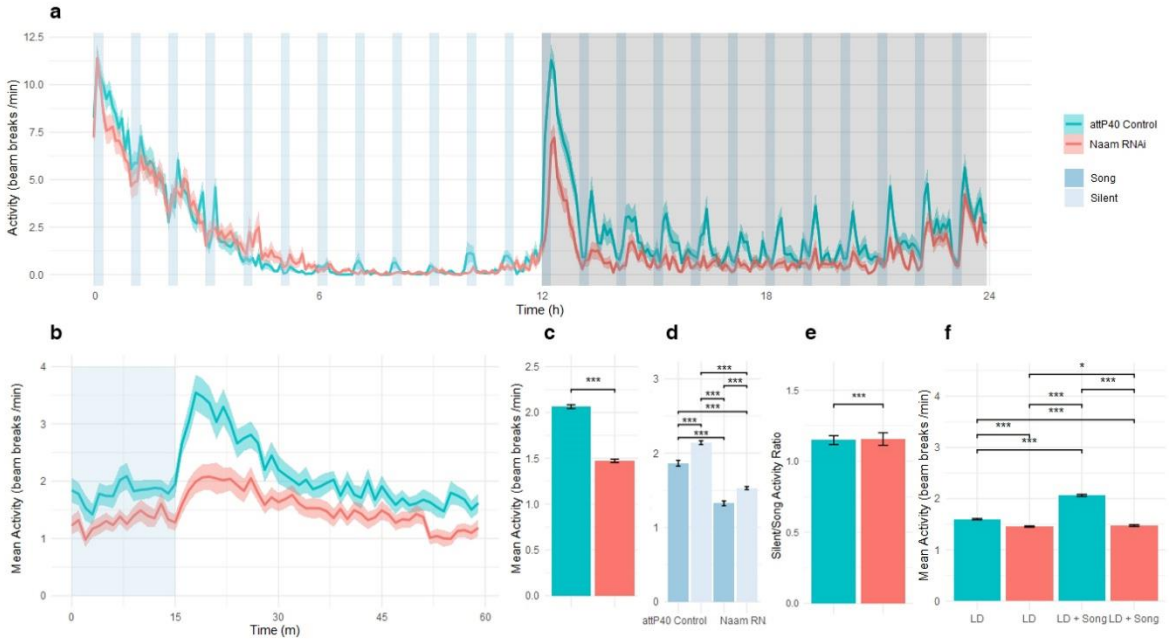


*Figure 8: Activity comparisons for the LD+Song phase. a) Line plots of mean genotype activity with respect to ZT at five-minute time resolution. Blue shaded rectangles show durations of song-stimulus presentation (15 minutes per hour). b) The 'average hour: Line plots of mean genotype activity with respect to time at one-minute time resolution, averaged over 24 hours to normalise circadian activity fluctuations. The blue shaded rectangle delineates the duration of the song-stimulus presentation (first quarter of each hour). As in the LD phase, mutant flies have a lower activity baseline. Paradoxically, no increase in activity is seen during presentation of the stimulus, but stimulus offset mediates a transient increase in activity. c) Mutant flies have a lower activity baseline compared to control flies throughout the LD+Song phase (mean difference=0.59 beam breaks/min, p<2.22e-16). d) Holm-Sidak-computed pairwise comparisons across genotypes and song/silence; all are significant at the p≤0.001 level. e) Silent/song activity ratio across genotypes; ratio difference=0.0073 (p<8.98e-11) in favour of mutants i.e., mutant flies are relatively more active during silence than song compared to the controls. f) Results of a two-way ANOVA comparing the LD phase of the experiment to the LD+Song phase across genotype (F(1,276637)=611.79, p<2.22e-16) with respect to effects on activity, revealing a significant interaction between experimental phase and genotype. Post-hoc analysis using the Holm-Sidak method revealed that the hourly stimulus increases overall activity in the controls (mean difference=0.46 breaks/min, p=4.79e-75) much more significantly than the mutants (0.017 breaks/min, p=0.023).*

## Discussion

This study set out to determine whether JO-restricted *Naam* knockdown disrupts circadian auditory gating and overall auditory function as indexed by the parameters of power gain, best frequency, and tuning sharpness. We used the TARGET system in an ectotherm. Ectothermic auditory systems are highly biophysically[49] and neurophysiologically[50] temperature-sensitive, both acutely and with acclimation (for evidence in *Drosophila* see ref.[51] S1). Hence, we structured our antennal measurement experiment to test across rearing temperatures as well as genotypes to disambiguate the effects of silencing *Naam* from auditory temperature acclimation, which is not of primary interest, though relevant for our data assessment.

*Naam* knockdown appears to increase the amplitude of circadian modulation of best frequency, but only in flies reared at 25 °C (Figure 4d) – clearly, this temperature is not perfectly Gal80$^{ts}$ restrictive (also observed in ref.[52]). A similar effect may manifest at 30 °C but be masked by the effects of increased rearing temperature. Interestingly, this accords with (non-significant) observations for power gain, where *Naam* knockdown appears to introduce a circadian rhythm to a previously arrhythmic parameter across temperatures. Nevertheless, although not observed at statistically significant magnitudes, best frequency modulations necessitate causative power gain

modulations under the assumption[24] that the antenna behaves as a simple harmonic oscillator with an actively regulated stiffness. Adjusting our model parameters may address this discrepancy.

LDV assays were methodologically limited by several factors. Firstly, the mounting procedure is irreversible and (eventually) lethal, contraindicating a repeated-measures study design. This necessitates greater cohorts, but introduces the problem that inter-individual circadian auditory variations are likely greater than intra-individual variations (circadian locomotor rhythms significantly vary inter-individually in amplitude[53] and phase[54]). Hence, as circadian auditory rhythms – individual-endogenous phenomena – must be analysed at a group level, the observed effect size is diminished. Additionally, without repeated measures, a stable, periodic, individual circadian rhythm cannot be tested directly, but may only be inferred as a group effect of entrainment. Furthermore, $CO_2$ anaesthesia across all experiments and ice sedation prior to LDV recordings both significantly alter *Drosophila*'s physiology[55 56 57 58]. However, our protocols were specifically designed to minimise this physiological impact.

This study falsifies its primary null hypothesis, showing that *Naam* knockdown influences auditory circadian rhythms. While the observed effect is small, there is reason to believe it may be greater under more physiological conditions. The *yw* genetic background flies assayed exhibited markedly diminished auditory rhythm amplitudes compared to Canton S flies (of particular note was an abnormal tuning sharpness arrhythmicity)[16]. Such variation is unsurprising in a complex trait such as circadian rhythm. A study of ~150 *Drosophila* strains observed continuous variation in six complex traits, with extreme values for each differing by more than four standard deviations[59]. Such variation contraindicates the study of particular objects with particular strains, such as neurodegeneration in $w^{1118}$ [60]. Indeed, attP40 and its insertion derivatives act as *MSP300* (a *Nesprin-1* orthologue[61]) insertional mutations, potentially invalidating their use for the study of myocytes[62]. This poses the serious concern that many attP40 RNAi screens are also *MSP300* enhancer screens.

Additionally, attP40, like other attP genome insertions, displays significant tissue-dependent expression variation, rendering it unsuitable for the study of certain tissues[63], although for JO these fears are allayed by our reporter images, and by both high attP40 expression in the JO15 neuron subset[64] and the ~94% labelling of JO neurons by NP0761 (ref.[65] S1). However, ref.[65] also documents ectopic central nervous system NP0761-Gal4 expression (as in other Gal4 lines[66]), which may partly explain the mutants' reduced locomotor activity. Finally, it cannot be excluded that the knockdown itself is cyclic; whether the attP40 locus or its flanking genes, *MSP300* and *CG14354,* are under circadian regulation is unknown. Estimates for the circadian-regulated transcriptome in *Drosophila* range from 6%[67 68] to 12.5%[69] of the genome (all putatively under *clk* control; *Drosophila* likely has no *clk*-independent circadian systems[70]). In *Arabidopsis*, this proportion is – similarly – 6%[71], and this translates to circadian-regulated transcription in 36% of *Arabidopsis* enhancer trap lines[72]. Nevertheless, transcriptional activity and mRNA abundance are not rigidly coupled. A nuanced dissection of these biochemical considerations is far beyond the scope of this study. Thus, knockdown has been assumed to be largely tissue specific and circadian-invariant.

Given the differences observed against Canton S, the *Naam* mutant phenotype may be background-dependent. Examples of this phenomenon abound in *Drosophila*[73]. Notably, heterozygous mutations in *Indy* observed to almost double lifespan[74] were later ascertained to produce their effects via genetic background interactions[75]. Similarly, phenotypic expressivity of the $scalloped^{E3}$ mutation is background-dependent[76]. This interaction has been experimentally

leveraged; comparison of *mbm* mutant phenotypes across different backgrounds revealed two genetic roles: one neurodevelopmental, the other in associated olfactory learning[77]. Nonetheless, *Drosophila* research remains relatively underdeveloped in its understanding of background-dependence, with no 'wild-type' standard, unlike with *C. elegans*[78], yeast[79], and mice[80]. Researchers working with these organisms directly transfect or introgress mutations into these respective stocks prior to detailed analysis[73]. The mouse community in particular has made great strides in establishing the examination of phenotypes in multiple genetic backgrounds[81]. A particularly illustrative study crossed *Cacna1c*$^{-/-}$ and *Tcf7l2*$^{-/-}$ male C57BL/6J mice with wild-type females from 30 inbred laboratory strains, finding extremely strong background interactions in the $F_1$ generation that sometimes supported diametrically opposing conclusions[82]. Hence, genetic background limits generalisability of genotype-phenotype relationships.

*Naam* knockdown presumptively attenuates *Naam* [mRNA] rhythms, but introduces a best frequency circadian rhythm, suggesting that the import of *Naam* varies with circadian time. This implies a complex, nonlinear interaction of *Naam* with its upstream regulators and protein-interaction partners, to which it may be epistatic. Any discussion of *Naam*'s precise role is speculative given the evidence in *Drosophila*. However, clock-driven transcription of the vertebrate orthologue *Nampt* drives circadian oscillation of NAD+. This rhythmically drives SIRT1 and SIRT3. SIRT1 feeds back to the key circadian transcription factors CLOCK/BMAL1, sustaining the circadian oscillation of NAD+. SIRT3 mediates circadian deacetylation of mitochondrial oxidative enzymes, regulating oxidative metabolism in mitochondria. Reduced NAMPT expression is thought to underlie decreased NAD+ biosynthesis and consequent age-related decline. NAD+ deficiency causes a pseudohypoxic state through decreased SIRT1 activity, disrupting nuclear-mitochondrial communication[83]. Thus, clock-driven *Naam*-dependent oscillations of the NAD+/NADH ratio may regulate oxidative metabolism rates in a sirtuin-dependent manner, with effects on energetic processes such as homeostasis. JO-targeted *Naam* knockdown may interfere with this regulation and accelerate auditory ageing. This consists with our falsification of our secondary null hypothesis which maps identically to the changes seen in the three auditory parameters during ARHL[21].

With respect to our behavioural observations, mutant activity deficits may be explained by impairments to the proprioceptive functions of JO, mediated by ~50% of the ~500 JO neurons[84], although this has not been documented for spontaneous activity. A mutant day/night activity ratio of ~2.5:1 (~1:1 in our controls) in the absence of auditory or vibratory stimuli is extremely difficult to explain by JO's auditory and proprioceptive roles. This points to a wider role for JO sensory inputs in activity homeostasis, consistent with the effects seen after antennal ablation[85]. Alternatively, attenuated a2 thermoreception (via *pyrexia*-expressing cap cells)[86 87 88] may underlie a failure of the mutants to appropriately shift their activity into the night, as classically observed under comparably high temperatures[89 90]. This could be experimentally verified with low-amplitude temperature-cycle entrainment under constant darkness.

Owing to its many functions, JO mediates increases in locomotor activity (as observed in males' responses to the courtship song[91]) as well as decreases (as seen in wind-induced suppression of locomotion[84]). The males we tested likely do not detect our mating-song stimulus as such given that their responses diverge from prior observations[92]. This may be a function of the amplitude and of the delivery method, in which vibrations were both air- and substrate-borne. Activity dynamics far more closely resemble – but do not perfectly match – dynamics observed in a study of vibration-induced sleep (VIS), where a 200Hz stimulus (a frequency close to our stimulus) mediates unchanged or decreased activity relative to baseline (cf. Canton S VIS), followed by a

'negative rebound' (activity peak). Negative rebounds aid the explanation of low-temporal resolution dynamics, where our stimulus increases 24hr activity far more in the controls compared to the mutants (Figure 8f). This implicates attenuated JO function, though not a particular JO neuron subgroup. However, responses were unlikely to be mediated solely by JO; NP0761-Gal4 has been shown to label the femoral chordotonal organ[93]. A more delicate understanding of *Naam*'s role in circadian auditory gating would be conferred by increasing the knockdown's spatial precision, delivering the stimulus at lower amplitudes using speakers, and conducting finer time-series analyses of activity and sleep.

In designing our auditory rhythm experiment, whilst we anticipated temperature-dependent effects, we neither anticipated their magnitude nor their complexity (i.e., temperature was observed to phase-shift the best frequency rhythm, as observed for locomotor rhythm[89]). Thus, the study design could be improved by exploiting non-temperature-dependent inducible gene-expression systems, such as the hormone-inducible Gene-Switch[94]. Developmental geneticists often use allelic series ranging from hypomorphic to amorphic to interrogate the gene structure/function relationship[76]. This may be replicated by combining Gene-Switch with multiple hormone concentrations[95] and overexpression constructs as well as knockdown constructs. In addition, isogenised (to ameliorate inter-individual rhythm variance) Canton S lines may provide an ideal background as they are known to exhibit strong auditory rhythms and have a well-characterised JO circadian-variable transcriptome. This could be combined with a battery of analyses, including antennal measurements but also extending to electrophysiological and behavioural (e.g. mating song response, egg-laying) assays. Auditory nerve calcium imaging may even allow for a repeated-measures design[64]. Exploration of the putatively homeostatic *Naam* should also occur at the extremes of age. The positioning of *Naam* downstream of four independent master regulators suggests it is part of a highly redundant system[21] (though does not preclude the possibility that it plays a non-redundant role). Thus, a simple loss-of-function analysis may be insufficiently powered to ascertain what effect *Naam* plays in *Drosophila's* auditory circadian rhythm. Elucidating this complex trait may be better served by forward genetic screens for auditory arrhythmic and hyperrhythmic fly lines, followed by statistical techniques such as quantitative trait locus mapping, rather than classical genetics methods.

## References


1. Albert, J. T., Nadrowski, B. & Göpfert, M. C. Mechanical signatures of transducer gating in the Drosophila ear. *Curr Biol* **17**, 1000–1006 (2007).
2. Nadrowski, B., Albert, J. T. & Göpfert, M. C. Transducer-Based Force Generation Explains Active Process in Drosophila Hearing. *Current Biology* **18**, 1365–1372 (2008).
3. Kamikouchi, A. *et al.* The neural basis of Drosophila gravity-sensing and hearing. *Nature* **458**, 165–171 (2009).
4. Jarman, A. P., Grell, E. H., Ackerman, L., Jan, L. Y. & Jan, Y. N. atonal is the proneural gene for Drosophila photoreceptors. *Nature* **369**, 398–400 (1994).
5. Wang, V. Y., Hassan, B. A., Bellen, H. J. & Zoghbi, H. Y. Drosophila atonal Fully Rescues the Phenotype of Math1 Null Mice: New Functions Evolve in New Cellular Contexts. *Current Biology* **12**, 1611–1616 (2002).
6. Weinberger, S. *et al.* Evolutionary changes in transcription factor coding sequence quantitatively alter sensory organ development and function. *eLife* **6**, e26402 (2017).
7. Göpfert, M. C. & Robert, D. The mechanical basis of Drosophila audition. *Journal of Experimental Biology* **205**, 1199–1208 (2002).

8. Matsuo, E. *et al.* Identification of novel vibration- and deflection-sensitive neuronal subgroups in Johnston's organ of the fruit fly. *Frontiers in Physiology* **5**, (2014).
9. Karak, S. *et al.* Diverse Roles of Axonemal Dyneins in Drosophila Auditory Neuron Function and Mechanical Amplification in Hearing. *Sci Rep* **5**, 17085 (2015).
10. Mackay, T. F. C. *et al.* Genetics and genomics of Drosophila mating behavior. *Proceedings of the National Academy of Sciences* **102**, 6622–6629 (2005).
11. Zhu, B., Sun, X., Zhang, H., Tang, Y. & Cui, J. Circadian Rhythm and Intersexual Differences in Auditory Frequency Sensitivity in Emei Music Frogs. *Asian Herpetological Research* **13**, 43–52 (2022).
12. Basinou, V., Park, J., Cederroth, C. R. & Canlon, B. Circadian regulation of auditory function. *Hearing Research* **347**, 47–55 (2017).
13. Yang, C.-H. *et al.* Constant Light Dysregulates Cochlear Circadian Clock and Exacerbates Noise-Induced Hearing Loss. *International Journal of Molecular Sciences* **21**, 7535 (2020).
14. Chabot, C. C. & Taylor, D. H. Circadian modulation of the rat acoustic startle response. *Behavioral Neuroscience* **106**, 846–852 (1992).
15. Frankland, P. W. & Ralph, M. R. Circadian modulation in the rat acoustic startle circuit. *Behavioral Neuroscience* **109**, 43–48 (1995).
16. Sudland, O. Circadian modulation in the antennal ear of Drosophila melanogaster. (University College London, 2021).
17. Barlow, R. Chapter 35 Circadian and efferent modulation of visual sensitivity. in *Progress in Brain Research* vol. 131 487–503 (Elsevier, 2001).
18. Grimaldi, B. *et al.* Chromatin remodeling and circadian control: master regulator CLOCK is an enzyme. *Cold Spring Harb Symp Quant Biol* **72**, 105–112 (2007).
19. Jauregui-Lozano, J. *et al.* The Clock:Cycle complex is a major transcriptional regulator of Drosophila photoreceptors that protects the eye from retinal degeneration and oxidative stress. *PLOS Genetics* **18**, e1010021 (2022).
20. Harper, R. E. F. 'Time Flies' Multisensory Processing by Circadian Clocks in Drosophila melanogaster. (University College London, 2017).
21. Keder, A. *et al.* Homeostatic maintenance and age-related functional decline in the Drosophila ear. *Sci Rep* **10**, 7431 (2020).
22. FlyBase Gene Report: Dmel\Naam. http://flybase.org/reports/FBgn0051216#expression.
23. Li, T., Bellen, H. J. & Groves, A. K. Using Drosophila to study mechanisms of hereditary hearing loss. *Disease Models & Mechanisms* **11**, dmm031492 (2018).
24. Albert, J. T. & Göpfert, M. C. Hearing in Drosophila. *Curr Opin Neurobiol* **34**, 79–85 (2015).
25. Albert, J. T. & Kozlov, A. S. Comparative Aspects of Hearing in Vertebrates and Insects with Antennal Ears. *Current Biology* **26**, R1050–R1061 (2016).
26. Göpfert, M. C. & Robert, D. Motion generation by Drosophila mechanosensory neurons. *Proceedings of the National Academy of Sciences* **100**, 5514–5519 (2003).
27. The Nobel Prize in Physiology or Medicine 2017. *NobelPrize.org* https://www.nobelprize.org/prizes/medicine/2017/press-release/.
28. Szklarczyk, D. *et al.* The STRING database in 2021: customizable protein–protein networks, and functional characterization of user-uploaded gene/measurement sets. *Nucleic Acids Research* **49**, D605–D612 (2021).
29. Balan, V. *et al.* Life span extension and neuronal cell protection by Drosophila nicotinamidase. *J Biol Chem* **283**, 27810–27819 (2008).
30. Lin, S.-J. & Guarente, L. Nicotinamide adenine dinucleotide, a metabolic regulator of transcription, longevity and disease. *Current Opinion in Cell Biology* **15**, 241–246 (2003).

31. Frankel, S., Ziafazeli, T. & Rogina, B. dSir2 and longevity in Drosophila. *Experimental Gerontology* **46**, 391–396 (2011).
32. Levine, D. C. *et al.* NADH inhibition of SIRT1 links energy state to transcription during time-restricted feeding. *Nat Metab* **3**, 1621–1632 (2021).
33. Rutter, J., Reick, M., Wu, L. C. & McKnight, S. L. Regulation of Clock and NPAS2 DNA Binding by the Redox State of NAD Cofactors. *Science* **293**, 510–514 (2001).
34. Poljsak, B. & Milisav, I. NAD+ as the Link Between Oxidative Stress, Inflammation, Caloric Restriction, Exercise, DNA Repair, Longevity, and Health Span. *Rejuvenation Research* **19**, 406–413 (2016).
35. van der Horst, A., Schavemaker, J. M., Pellis-van Berkel, W. & Burgering, B. M. T. The Caenorhabditis elegans nicotinamidase PNC-1 enhances survival. *Mechanisms of Ageing and Development* **128**, 346–349 (2007).
36. Rivas-Chacón, L. del M. *et al.* Role of Oxidative Stress in the Senescence Pattern of Auditory Cells in Age-Related Hearing Loss. *Antioxidants (Basel)* **10**, 1497 (2021).
37. McGuire, S. E., Le, P. T., Osborn, A. J., Matsumoto, K. & Davis, R. L. Spatiotemporal Rescue of Memory Dysfunction in Drosophila. *Science* **302**, 1765–1768 (2003).
38. Pézier, A. & Blagburn, J. M. Auditory Responses of Engrailed and Invected-Expressing Johnston's Organ Neurons in Drosophila melanogaster. *PLoS One* **8**, e71419 (2013).
39. Perkins, L. *et al.* The Transgenic RNAi Project at Harvard Medical School: Resources and Validation. *Genetics* **201**, (2015).
40. Göpfert, M. C., Humphris, A. D. L., Albert, J. T., Robert, D. & Hendrich, O. Power gain exhibited by motile mechanosensory neurons in Drosophila ears. *Proceedings of the National Academy of Sciences* **102**, 325–330 (2005).
41. Tuning Curve - an overview | ScienceDirect Topics. https://www.sciencedirect.com/topics/nursing-and-health-professions/tuning-curve.
42. Wobbrock, J. O., Findlater, L., Gergle, D. & Higgins, J. J. The aligned rank transform for nonparametric factorial analyses using only anova procedures. in *Proceedings of the SIGCHI Conference on Human Factors in Computing Systems* 143–146 (Association for Computing Machinery, 2011). doi:10.1145/1978942.1978963.
43. Elkin, L. A., Kay, M., Higgins, J. J. & Wobbrock, J. O. An Aligned Rank Transform Procedure for Multifactor Contrast Tests. in *The 34th Annual ACM Symposium on User Interface Software and Technology* 754–768 (Association for Computing Machinery, 2021). doi:10.1145/3472749.3474784.
44. Introduction.
45. Geissmann, Q., Rodriguez, L. G., Beckwith, E. J. & Gilestro, G. F. Rethomics: An R framework to analyse high-throughput behavioural data. *PLOS ONE* **14**, e0209331 (2019).
46. Bustin, S. A. *et al.* The MIQE Guidelines: Minimum Information for Publication of Quantitative Real-Time PCR Experiments. *Clinical Chemistry* **55**, 611–622 (2009).
47. Bennet-Clark, H. C. Acoustics of Insect Song. *Nature* **234**, 255–259 (1971).
48. Grima, B., Chélot, E., Xia, R. & Rouyer, F. Morning and evening peaks of activity rely on different clock neurons of the Drosophila brain. *Nature* **431**, 869–873 (2004).
49. Eberhard, M. J. B., Gordon, S. D., Windmill, J. F. C. & Ronacher, B. Temperature effects on the tympanal membrane and auditory receptor neurons in the locust. *J Comp Physiol A Neuroethol Sens Neural Behav Physiol* **200**, 837–847 (2014).
50. Wysocki, L. E., Montey, K. & Popper, A. N. The influence of ambient temperature and thermal acclimation on hearing in a eurythermal and a stenothermal otophysan fish. *Journal of Experimental Biology* **212**, 3091–3099 (2009).

51. Boyd-Gibbins, N. *et al.* Turnover and activity-dependent transcriptional control of NompC in the Drosophila ear. *iScience* **24**, 102486 (2021).
52. Zeidler, M. P. *et al.* Temperature-sensitive control of protein activity by conditionally splicing inteins. *Nat Biotechnol* **22**, 871–876 (2004).
53. Wu, K. J., Kumar, S., Serrano Negron, Y. L. & Harbison, S. T. Genotype Influences Day-to-Day Variability in Sleep in Drosophila melanogaster. *Sleep* **41**, zsx205 (2017).
54. Srivastava, M., Varma, V., Abhilash, L., Sharma, V. K. & Sheeba, V. Circadian Clock Properties and Their Relationships as a Function of Free-Running Period in Drosophila melanogaster. *J Biol Rhythms* **34**, 231–248 (2019).
55. MacMillan, H. A., Andersen, J. L., Davies, S. A. & Overgaard, J. The capacity to maintain ion and water homeostasis underlies interspecific variation in Drosophila cold tolerance. *Sci Rep* **5**, 18607 (2015).
56. Bartholomew, N. R., Burdett, J. M., VandenBrooks, J. M., Quinlan, M. C. & Call, G. B. Impaired climbing and flight behaviour in Drosophila melanogaster following carbon dioxide anaesthesia. *Sci Rep* **5**, 15298 (2015).
57. Roy, M., Sivan-Loukianova, E. & Eberl, D. F. Cell-type-specific roles of Na+/K+ ATPase subunits in Drosophila auditory mechanosensation. *Proc Natl Acad Sci U S A* **110**, 181–186 (2013).
58. Barron, A. B. Anaesthetising Drosophila for behavioural studies. *Journal of Insect Physiology* **46**, 439–442 (2000).
59. Evangelou, A. *et al.* Unpredictable Effects of the Genetic Background of Transgenic Lines in Physiological Quantitative Traits. *G3 (Bethesda)* **9**, 3877–3890 (2019).
60. Ferreiro, M. J. *et al.* Drosophila melanogaster White Mutant w1118 Undergo Retinal Degeneration. *Frontiers in Neuroscience* **11**, (2018).
61. Zhang, Q., Ragnauth, C., Greener, M. J., Shanahan, C. M. & Roberts, R. G. The Nesprins Are Giant Actin-Binding Proteins, Orthologous to Drosophila melanogaster Muscle Protein MSP-300. *Genomics* **80**, 473–481 (2002).
62. Graaf, K. van der, Srivastav, S., Singh, P., McNew, J. A. & Stern, M. The Drosophila attP40 docking site and derivatives are insertion mutations of MSP300. 2022.05.14.491875 Preprint at https://doi.org/10.1101/2022.05.14.491875 (2022).
63. Markstein, M., Pitsouli, C., Villalta, C., Celniker, S. E. & Perrimon, N. Exploiting position effects and the gypsy retrovirus insulator to engineer precisely expressed transgenes. *Nat Genet* **40**, 476–483 (2008).
64. Kay, A. R. *et al.* Goggatomy: A Method for Opening Small Cuticular Compartments in Arthropods for Physiological Experiments. *Frontiers in Physiology* **7**, (2016).
65. Schoen, C. J. *et al.* Increased activity of Diaphanous homolog 3 (DIAPH3)/diaphanous causes hearing defects in humans with auditory neuropathy and in Drosophila. *Proceedings of the National Academy of Sciences* **107**, 13396–13401 (2010).
66. Casas-Tintó, S., Arnés, M. & Ferrús, A. Drosophila enhancer-Gal4 lines show ectopic expression during development. *Royal Society Open Science* **4**, 170039.
67. Stempfl, T. *et al.* Identification of Circadian-Clock-Regulated Enhancers and Genes of Drosophila melanogaster by Transposon Mobilization and Luciferase Reporting of Cyclical Gene Expression. *Genetics* **160**, 571–593 (2002).
68. Ueda, H. R. *et al.* Genome-wide Transcriptional Orchestration of Circadian Rhythms inDrosophila*210. *Journal of Biological Chemistry* **277**, 14048–14052 (2002).
69. Litovchenko, M. *et al.* Extensive tissue-specific expression variation and novel regulators underlying circadian behavior. *Sci Adv* **7**, eabc3781 (2021).

70. McDonald, M. J. & Rosbash, M. Microarray Analysis and Organization of Circadian Gene Expression in Drosophila. *Cell* **107**, 567–578 (2001).
71. Harmer, S. L. *et al.* Orchestrated transcription of key pathways in Arabidopsis by the circadian clock. *Science* **290**, 2110–2113 (2000).
72. Michael, T. P. & McClung, C. R. Enhancer Trapping Reveals Widespread Circadian Clock Transcriptional Control in Arabidopsis. *Plant Physiology* **132**, 629–639 (2003).
73. Wesley, E. R., Hawley, R. S. & Billmyre, K. K. Genetic background impacts the timing of synaptonemal complex breakdown in Drosophila melanogaster. *Chromosoma* **129**, 243–254 (2020).
74. Rogina, B., Reenan, R. A., Nilsen, S. P. & Helfand, S. L. Extended Life-Span Conferred by Cotransporter Gene Mutations in Drosophila. *Science* **290**, 2137–2140 (2000).
75. Toivonen, J. M. *et al.* No Influence of Indy on Lifespan in Drosophila after Correction for Genetic and Cytoplasmic Background Effects. *PLOS Genetics* **3**, e95 (2007).
76. Dworkin, I. *et al.* Genomic Consequences of Background Effects on scalloped Mutant Expressivity in the Wing of Drosophila melanogaster. *Genetics* **181**, 1065–1076 (2009).
77. de Belle, J. S. & Heisenberg, M. Expression of Drosophila mushroom body mutations in alternative genetic backgrounds: a case study of the mushroom body miniature gene (mbm). *Proc Natl Acad Sci U S A* **93**, 9875–9880 (1996).
78. Sterken, M. G., Snoek, L. B., Kammenga, J. E. & Andersen, E. C. The laboratory domestication of Caenorhabditis elegans. *Trends in Genetics* **31**, 224–231 (2015).
79. Mortimer, R. K. & Johnston, J. R. Genealogy of principal strains of the yeast genetic stock center. *Genetics* **113**, 35–43 (1986).
80. Sarsani, V. K. *et al.* The Genome of C57BL/6J "Eve", the Mother of the Laboratory Mouse Genome Reference Strain. *G3 Genes|Genomes|Genetics* **9**, 1795–1805 (2019).
81. Justice, M. J. & Dhillon, P. Using the mouse to model human disease: increasing validity and reproducibility. *Disease Models & Mechanisms* **9**, 101–103 (2016).
82. Sittig, L. J. *et al.* Genetic Background Limits Generalizability of Genotype-Phenotype Relationships. *Neuron* **91**, 1253–1259 (2016).
83. Imai, S. & Guarente, L. It takes two to tango: NAD+ and sirtuins in aging/longevity control. *npj Aging Mech Dis* **2**, 1–6 (2016).
84. Yorozu, S. *et al.* Distinct sensory representations of wind and near-field sound in the Drosophila brain. *Nature* **458**, 201–205 (2009).
85. Simoni, A. *et al.* A Mechanosensory Pathway to the Drosophila Circadian Clock. *Science* **343**, 525–528 (2014).
86. George, R. & Stanewsky, R. Peripheral Sensory Organs Contribute to Temperature Synchronization of the Circadian Clock in Drosophila melanogaster. *Front Physiol* **12**, 622545 (2021).
87. Roessingh, S. *et al.* Temperature synchronization of the Drosophila circadian clock protein PERIOD is controlled by the TRPA channel PYREXIA. *Commun Biol* **2**, 246 (2019).
88. Wolfgang, W., Simoni, A., Gentile, C. & Stanewsky, R. The Pyrexia transient receptor potential channel mediates circadian clock synchronization to low temperature cycles in Drosophila melanogaster. *Proc Biol Sci* **280**, 20130959 (2013).
89. Majercak, J., Sidote, D., Hardin, P. E. & Edery, I. How a Circadian Clock Adapts to Seasonal Decreases in Temperature and Day Length. *Neuron* **24**, 219–230 (1999).
90. Ishimoto, H., Lark, A. & Kitamoto, T. Factors that Differentially Affect Daytime and Nighttime Sleep in Drosophila melanogaster. *Front Neurol* **3**, 24 (2012).
91. Kowalski, S., Aubin, T. & Martin, J.-R. Courtship song in Drosophila melanogaster: a differential effect on male–female locomotor activity. *Can. J. Zool.* **82**, 1258–1266 (2004).

92. Kashkenbayeva, Assel. Modulators of Auditory Responses in Drosophila: From the Ear to Behaviour via the Clock? (University College London, 2020).
93. Wiek, R. A Functional Characterisation of Drosophila Chordotonal Organs. (Universität Göttingen, 2013).
94. McGuire, S. E., Mao, Z. & Davis, R. L. Spatiotemporal Gene Expression Targeting with the TARGET and Gene-Switch Systems in Drosophila. *Science's STKE* **2004**, pl6–pl6 (2004).
95. Poirier, L., Shane, A., Zheng, J. & Seroude, L. Characterization of the Drosophila Gene-Switch system in aging studies: a cautionary tale. *Aging Cell* **7**, 758–770 (2008).
96. Damulewicz, M. *et al.* Clock and clock-controlled genes are differently expressed in the retina, lamina and in selected cells of the visual system of Drosophila melanogaster. *Frontiers in Cellular Neuroscience* **9**, (2015).
97. Livak, K. J. & Schmittgen, T. D. Analysis of relative gene expression data using real-time quantitative PCR and the 2(-Delta Delta C(T)) Method. *Methods* **25**, 402–408 (2001).
98. Rudic, R. D. *et al.* BMAL1 and CLOCK, two essential components of the circadian clock, are involved in glucose homeostasis. *PLoS Biol* **2**, e377 (2004).
99. Hughes, M. E. *et al.* Harmonics of circadian gene transcription in mammals. *PLoS Genet* **5**, e1000442 (2009).
100. GTEx Consortium. The Genotype-Tissue Expression (GTEx) project. *Nat Genet* **45**, 580–585 (2013).
101. CIRCA: Circadian gene expression profiles. http://circadb.hogeneschlab.org/human.
102. Levine, D. C. *et al.* NAD+ Controls Circadian Reprogramming through PER2 Nuclear Translocation to Counter Aging. *Molecular Cell* **78**, 835-849.e7 (2020).
103. Peek, C. B., Ramsey, K. M., Marcheva, B. & Bass, J. Nutrient sensing and the circadian clock. *Trends in Endocrinology & Metabolism* **23**, 312–318 (2012).
104. Lighton, J. R. B. Respiratory Physiology: Strange Cycles and the Fruit-Fly's Tongue. *Current Biology* **15**, R965–R966 (2005).
105. Lehmann, F.-O. & Heymann, N. Unconventional mechanisms control cyclic respiratory gas release in flying Drosophila. *Journal of Experimental Biology* **208**, 3645–3654 (2005).

# Appendix

## A Pilot Quantitative Reverse Transcription Polymerase Chain-reaction (RT-qPCR) Tentatively Confirms Circadian-time-dependent *Naam* Expression and RNAi-mediated Knockdown

RNA from entrained 12-day-old *Naam* RNAi and attP40 control flies was extracted for RT-qPCR to analyse circadian changes of *Naam* and predicted *Naam* interactome components (see methods). A two-way ANOVA to analyse the effects of genotype and zeitgeber time on *Naam* cycle threshold (Ct) value revealed no statistically significant interaction between the effects of genotype and zeitgeber time ($F(1, 8)=4.593$, $p=0.0645$). Simple main effects analysis showed that both genotype ($F(1, 8)=71.874$, $p=2.87e-05$) and zeitgeber time ($F(3, 8)=7.457$, $p=0.0258$) have a statistically significant effect on Ct. Pairwise comparisons were conducted between all groups using the Tukey HSD method and are shown in

Figure 9.

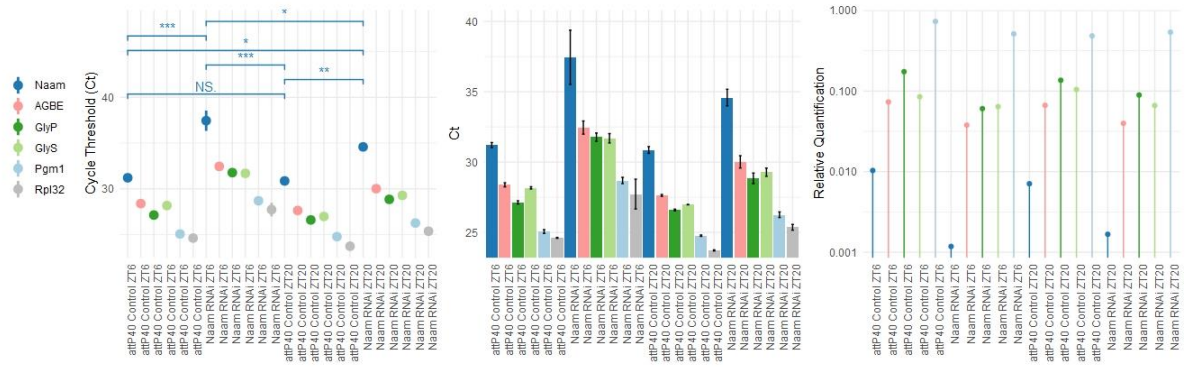


*Figure 9: Expression changes for* Naam *and predicted interaction partners in both* Naam *RNAi and attP40 control animals at ZT6 and ZT20, the predicted maximum and minimum (respectively) of the periodic function relating* Naam *mRNA concentration to zeitgeber time. Left panel: points show mean target Ct values across experimental conditions, error bars show the SEM. Pairwise comparisons for* Naam *Ct were done using the Tukey method. Notably, the mutant flies'* Naam *Ct values are higher than their control counterparts (respective mean differences for ZT6 and ZT20: 6.25 (p=3.15e-4) and 3.73 (p=8.87e-3) indicating partial knockdown of Naam. Additionally,* Naam *Ct value varied significantly between timepoints for the mutants (2.87, p=0.0356) but not the controls (0.35, p=0.974). Middle panel: as per left panel with columns and error bars more clearly showing means and SEMs. Right panel: relative quantification values for all targets normalised against* Rpl32 *(a circadian-time-stable housekeeping gene); note logarithmic axis.*

## Methods: RT-qPCR

*Naam* RNAi flies and attP40 controls were entrained to a 12:12hr light:dark (LD) cycle at 30°C and 70% RH. On their 12th day they were frozen in liquid nitrogen at the respective timepoints of interest and then stored at -80°C. Four male flies, composing one biological replicate, were homogenised in lysis buffer containing 1% β-mercaptoethanol). RNA was immediately extracted (as per the Qiagen RNeasy Mini Kit protocol) and reverse transcription carried out using the High-Capacity RNA to cDNA kit (Applied Biosystems) protocol. Taqman primers were pre-mixed and contained probes for *Naam, AGBE, GlyP, GlyS, Pgm1,* and *Rpl32*. *Ribosomal protein 32 (Rpl32)* was chosen as an endogenous control due to highly circadian-time-stable expression[96]. 0.5µL of primer mix was added to 4.5µL of master mix (Taqman) and 4.5µL of cDNA made up to 3ng/µL with nuclease-free water. The qPCR was performed on a Step One Plus ABI machine. The 96-well plate design was fed into the Step One Plus software. One biological replicate was performed per genotype per timepoint. Three technical replicates were run for each sample and each target, as well as three negative controls per target. Reactions were prepared per the TaqMan Gene Expression Assay protocol.

Cycle threshold (Ct) values were extracted from the Step One Plus software. The 2(-Delta Delta C(T)) method[97] was used to derive a relative quantification (RQ) value to analyse relative changes in gene expression against *Rpl32*. In brief,

$$\Delta Ct = Ct_{gene} \times control - Ct_{endogenous\ control}$$

$$\Delta\Delta Ct = \Delta Ct - (Ct_{gene} \times knockdown - Ct_{endogenous\ control})$$

$$RQ = 2^{-\Delta\Delta Ct} \qquad s = \sqrt{s_1^2 - s_2^2}$$

where $s$ is the error term, $s_1$ is the gene of interest, and $s_2$ is the reference gene. Statistical analysis was performed in R. Data were parametric; a two-way analysis of variance (ANOVA) was conducted alongside the Tukey HSD method for pairwise comparisons.

## Supplementary Figures

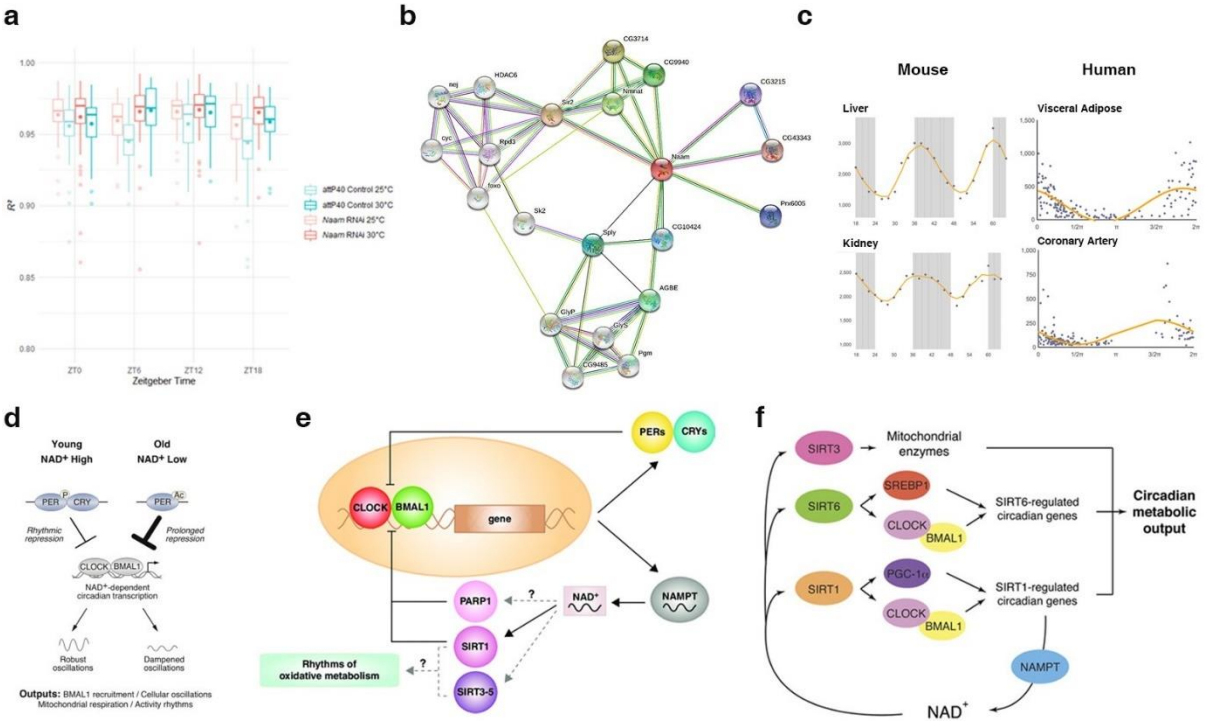


*Figure 10. a) Assessment of goodness of fit: $R^2$ values for 99.3% of fits to the fourier-transformed LDV recording dataset (n=962) exceeded 0.85. b) STRING database outputs for* Naam *protein interaction partners (ref.[28]). c) Nampt (the vertebrate orthologue of Naam) mRNA cycles in tissues in mice (liver[98], kidney[99]) and humans[100] (visceral adipose tissue, coronary artery). Figures are reproduced from a search query ("nampt") submitted to CircaDB, a database for circadian-cycling mammalian genes (ref.[101]). d) In old mice, a lower NAD+/NADH ratio leads to PER2 acetylation, ultimating in dampened BMAL1 chromatin binding rhythms, transcriptional oscillations, mitochondrial respiration rhythms, and activity rhythms [102]. e) Clock targets include metabolic genes, such as the NAD+ biosynthetic enzyme NAMPT. NAD+ is an essential cofactor for the metabolic regulators, SIRT1, SIRT3-5 and PARP1, which may control rhythms of oxidative metabolism (ref.[103]). f) Clock-driven NAMPT transcription drives circadian oscillation of NAD+. This rhythmically drives SIRT1, SIRT3, and SIRT6. SIRT1 feedbacks the key circadian transcription factors CLOCK/BMAL. SIRT1 may also regulate Bmal1 expression. SIRT3 mediates circadian deacetylation of mitochondrial oxidative enzymes, regulating oxidative metabolism in mitochondria. Thus, circadian activity of sirtuins produces metabolic rhythms across tissues (ref.[83]).*

## A Note on Methodological Limitations

$CO_2$ anaesthesia deleteriously alters respiratory and muscle physiology, producing flight and climbing deficits lasting days post-exposure[56]. Chill-coma induction is likely mediated by suppression of $Na^+/K^+$-ATPase below the threshold necessary to maintain ionic concentration gradients, ultimating in an increased haemolymph $[K^+]$ which depolarises cell resting potentials. RNAi-mediated-knockdown of JO-expressed ATPase subunits produces near-complete deafness[57]. Additionally, both methods (as well as mechanical shocks) increase copulation latency[58]. All these perturbations may precipitate strong physiological adaptations that mask low-amplitude circadian rhythms. Moreover, the LDV mounting procedure requires partial thoracic immobilisation. This is problematic given the risk of spiracle obstruction, which would inordinately impact *Drosophila's* tracheal respiratory system given its passive diffusion reliance[104 105]. The progressively deteriorating physiological state effected by the mounting procedure may well attenuate auditory circadian rhythms, given that they are mediated by power gain[2]. Nevertheless, as these limitations (theoretically) randomly distribute across independent variable levels, this should not compromise the validity of the results. Additionally, our protocol was specifically designed to ameliorate these deleterious impacts.

# Supplementary Data for LDV Antennal Assays

## Within Temperature-group Comparisons: 25°C

**Two-way ANOVA: Power Gain**

| Term | Df | Df.res | Sum Sq | Sum Sq.res | F value | Pr(>F) |
|---|---|---|---|---|---|---|
| Genotype | 1 | 470 | 1958783 | 7118290 | 129.3327 | 1.22E-26 |
| Zeitgeber Time | 3 | 470 | 128443.2 | 8961023 | 2.245588 | 0.082244 |
| Genotype:Zeitgeber Time | 3 | 470 | 67734.16 | 8999459 | 1.179147 | 0.317157 |

**Two-way ANOVA: Best Frequency**

| Term | Df | Df.res | Sum Sq | Sum Sq.res | F value | Pr(>F) |
|---|---|---|---|---|---|---|
| Genotype | 1 | 470 | 2065844.7 | 6693669.7 | 145.05451 | 2.66E-29 |
| Zeitgeber Time | 3 | 470 | 446408.28 | 8484959.4 | 8.2425023 | 2.35E-05 |
| Genotype:Zeitgeber Time | 3 | 470 | 163872.28 | 8718103.6 | 2.9448289 | 0.0326318 |

**Two-way ANOVA: Tuning Sharpness**

| Term | Df | Df.res | Sum Sq | Sum Sq.res | F value | Pr(>F) |
|---|---|---|---|---|---|---|
| Genotype | 1 | 470 | 11493.3700 | 8886251.99 | 0.60789227 | 0.43597494 |
| Zeitgeber Time | 3 | 470 | 118677.253 | 8757013.59 | 2.12318611 | 0.09646524 |
| Genotype:Zeitgeber Time | 3 | 470 | 89628.8490 | 8691617.06 | 1.61556278 | 0.1849131 |

Post-hoc pairwise comparisons using the Holm-Sidak correction are provided below, along with all respective contrast estimates and respective standard errors, t-ratios, and p-values.

## Within Temperature-group Comparisons: 30°C

**Two-way ANOVA: Power Gain**

| Term | Df | Df.res | Sum Sq | Sum Sq.res | F value | Pr(>F) |
|---|---|---|---|---|---|---|
| Genotype | 1 | 476 | 1927938.101 | 7346222.84 | 124.9211405 | 6.49E-26 |
| Zeitgeber Time | 3 | 476 | 226617.0906 | 9065253.65 | 3.96641724 | 0.008232093 |
| Genotype:Zeitgeber Time | 3 | 476 | 15494.34819 | 9232254.10 | 0.266287794 | 0.849698705 |

**Two-way ANOVA: Best Frequency**

| Term | Df | Df.res | Sum Sq | Sum Sq.res | F value | Pr(>F) |
|---|---|---|---|---|---|---|
| Genotype | 1 | 476 | 225018.5377 | 9204396.994 | 11.6367019 | 0.000701717 |
| Zeitgeber Time | 3 | 476 | 489634.2306 | 8950871.157 | 8.679449173 | 1.29E-05 |
| Genotype:Zeitgeber Time | 3 | 476 | 14961.02237 | 9412042.752 | 0.252210451 | 0.859763784 |

**Two-way ANOVA: Tuning Sharpness**

| Term | Df | Df.res | Sum Sq | Sum Sq.res | F value | Pr(>F) |
|---|---|---|---|---|---|---|
| Genotype | 1 | 476 | 430595.4195 | 8629209.701 | 23.7522817 | 1.49E-06 |
| Zeitgeber Time | 3 | 476 | 33409.3457 | 9226063.74 | 0.574562421 | 0.63196993 |
| Genotype:Zeitgeber Time | 3 | 476 | 27488.46432 | 9207610.613 | 0.473684562 | 0.700753944 |

Post-hoc pairwise comparisons using the Holm-Sidak correction are provided below, along with all respective contrast estimates and respective standard errors, t-ratios, and p-values.

## Within Genotype Comparisons: attP40 Controls

**Two-way ANOVA: Power Gain**

| Term | Df | Df.res | Sum Sq | Sum Sq.res | F value | Pr(>F) |
|---|---|---|---|---|---|---|
| Rearing Temperature | 1 | 475 | 385007.4605 | 8852583.521 | 20.65821162 | 6.97E-06 |
| Zeitgeber Time | 3 | 475 | 59082.5883 | 9192245.233 | 1.017677718 | 0.384516928 |
| Rearing Temperature:Zeitgeber Time | 3 | 475 | 18736.25191 | 9226317.045 | 0.321533848 | 0.809807928 |

**Two-way ANOVA: Best Frequency**

| Term | Df | Df.res | Sum Sq | Sum Sq.res | F value | Pr(>F) |
|---|---|---|---|---|---|---|
| Rearing Temperature | 1 | 475 | 3410498.045 | 5953809.17 | 272.092458 | 1.17E-48 |
| Zeitgeber Time | 3 | 475 | 179681.9893 | 9199261.975 | 3.092601165 | 0.026770898 |

| | | | | | | |
|---|---|---|---|---|---|---|
| Rearing Temperature:Zeitgeber Time | 3 | 475 | 218168.6572 | 9162444.563 | 3.770104199 | 0.010744145 |

**Two-way ANOVA: Tuning Sharpness**

| Term | Df | Df.res | Sum Sq | Sum Sq.res | F value | Pr(>F) |
|---|---|---|---|---|---|---|
| Rearing Temperature | 1 | 475 | 1340431.791 | 7840942.584 | 81.20262248 | 4.99E-18 |
| Zeitgeber Time | 3 | 475 | 79441.57329 | 8999733.914 | 1.397624555 | 0.242786587 |
| Rearing Temperature:Zeitgeber Time | 3 | 475 | 60929.90422 | 9031641.846 | 1.068159588 | 0.362226687 |

Post-hoc pairwise comparisons using the Holm-Sidak correction are provided below, along with all respective contrast estimates and respective standard errors, t-ratios, and p-values.

## Within Genotype Comparisons: Naam RNAi

**Two-way ANOVA: Power Gain**

| Term | Df | Df.res | Sum Sq | Sum Sq.res | F value | Pr(>F) |
|---|---|---|---|---|---|---|
| Rearing Temperature | 1 | 471 | 405906.4512 | 8626722.605 | 22.16159569 | 3.30E-06 |
| Zeitgeber Time | 3 | 471 | 541389.8692 | 8495251.234 | 10.00537914 | 2.10E-06 |
| Rearing Temperature:Zeitgeber Time | 3 | 471 | 19470.47293 | 9038060.802 | 0.338221253 | 0.797707819 |

**Two-way ANOVA: Best Frequency**

| Term | Df | Df.res | Sum Sq | Sum Sq.res | F value | Pr(>F) |
|---|---|---|---|---|---|---|
| Rearing Temperature | 1 | 471 | 1524214.595 | 7546797.783 | 95.12711151 | 1.36E-20 |
| Zeitgeber Time | 3 | 471 | 68818.11715 | 8960943.599 | 1.205726191 | 0.307125076 |
| Rearing Temperature:Zeitgeber Time | 3 | 471 | 675991.97 | 8325210.782 | 12.74811438 | 5.05E-08 |

**Two-way ANOVA: Tuning Sharpness**

| Term | Df | Df.res | Sum Sq | Sum Sq.res | F value | Pr(>F) |
|---|---|---|---|---|---|---|
| Rearing Temperature | 1 | 471 | 311593.1288 | 8257359.813 | 17.77327947 | 2.98E-05 |
| Zeitgeber Time | 3 | 471 | 39901.39729 | 8429370.829 | 0.743177575 | 0.526722029 |
| Rearing Temperature:Zeitgeber Time | 3 | 471 | 25338.79344 | 8360387.894 | 0.475838038 | 0.69924931 |

Post-hoc pairwise comparisons using the Holm-Sidak correction are provided below, along with all respective contrast estimates and respective standard errors, t-ratios, and p-values.

## Means for Power Gain, Best Frequency, and Tuning Sharpness

| Genotype | Zeitgeber Time | Rearing Temperature | Mean Power Gain | SEM | n= |
|---|---|---|---|---|---|
| Naam RNAi | ZT0 | 25°C | 4.07913 | 0.261754 | 60 |
| Naam RNAi | ZT0 | 30°C | 5.029779 | 0.309497 | 62 |
| Naam RNAi | ZT6 | 25°C | 4.522482 | 0.268214 | 60 |
| Naam RNAi | ZT6 | 30°C | 5.913981 | 0.485045 | 60 |
| Naam RNAi | ZT12 | 25°C | 4.153366 | 0.291509 | 60 |
| Naam RNAi | ZT12 | 30°C | 6.360529 | 0.569501 | 60 |
| Naam RNAi | ZT18 | 25°C | 3.187657 | 0.331121 | 57 |
| Naam RNAi | ZT18 | 30°C | 4.09982 | 0.253155 | 60 |
| attP40 Control | ZT0 | 25°C | 6.587174 | 0.34793 | 61 |
| attP40 Control | ZT0 | 30°C | 7.788876 | 0.348182 | 62 |
| attP40 Control | ZT6 | 25°C | 6.606583 | 0.327601 | 60 |
| attP40 Control | ZT6 | 30°C | 9.625621 | 0.779223 | 60 |
| attP40 Control | ZT12 | 25°C | 7.057147 | 0.484273 | 60 |
| attP40 Control | ZT12 | 30°C | 9.058386 | 0.577821 | 60 |
| attP40 Control | ZT18 | 25°C | 6.70312 | 0.453336 | 60 |
| attP40 Control | ZT18 | 30°C | 8.46266 | 0.706488 | 60 |
| **Genotype** | **Zeitgeber Time** | **Rearing Temperature** | **Mean Best Frequency** | **SEM** | **n=** |
| Naam RNAi | ZT0 | 25°C | 300.0421 | 2.894049 | 60 |
| Naam RNAi | ZT0 | 30°C | 353.8966 | 4.714083 | 62 |
| Naam RNAi | ZT6 | 25°C | 317.1166 | 4.401874 | 60 |
| Naam RNAi | ZT6 | 30°C | 356.6203 | 5.910566 | 60 |
| Naam RNAi | ZT12 | 25°C | 312.6385 | 4.274437 | 60 |
| Naam RNAi | ZT12 | 30°C | 362.5292 | 5.697845 | 60 |
| Naam RNAi | ZT18 | 25°C | 358.0018 | 12.06387 | 57 |
| Naam RNAi | ZT18 | 30°C | 336.8283 | 5.194345 | 60 |
| attP40 Control | ZT0 | 25°C | 271.4266 | 2.922829 | 61 |
| attP40 Control | ZT0 | 30°C | 336.8997 | 5.531697 | 62 |
| attP40 Control | ZT6 | 25°C | 278.1582 | 4.763009 | 60 |
| attP40 Control | ZT6 | 30°C | 333.7052 | 6.829478 | 60 |

| | | | | | |
|---|---|---|---|---|---|
| attP40 Control | ZT12 | 25°C | 283.3321 | 5.499439 | 60 |
| attP40 Control | ZT12 | 30°C | 353.0836 | 6.25007 | 60 |
| attP40 Control | ZT18 | 25°C | 282.8343 | 5.216733 | 60 |
| attP40 Control | ZT18 | 30°C | 322.374 | 4.938175 | 60 |
| **Genotype** | **Zeitgeber Time** | **Rearing Temperature** | **Mean Tuning Sharpness** | **SEM** | **n=** |
| Naam RNAi | ZT0 | 25°C | 1.53725 | 0.046993 | 60 |
| Naam RNAi | ZT0 | 30°C | 2.172179 | 0.132738 | 62 |
| Naam RNAi | ZT6 | 25°C | 1.677441 | 0.075024 | 60 |
| Naam RNAi | ZT6 | 30°C | 2.405129 | 0.225053 | 60 |
| Naam RNAi | ZT12 | 25°C | 1.786017 | 0.099747 | 60 |
| Naam RNAi | ZT12 | 30°C | 2.615595 | 0.28384 | 60 |
| Naam RNAi | ZT18 | 25°C | 1.767277 | 0.109356 | 57 |
| Naam RNAi | ZT18 | 30°C | 1.936945 | 0.120364 | 60 |
| attP40 Control | ZT0 | 25°C | 1.719414 | 0.103253 | 61 |
| attP40 Control | ZT0 | 30°C | 2.47531 | 0.144139 | 62 |
| attP40 Control | ZT6 | 25°C | 1.571496 | 0.077403 | 60 |
| attP40 Control | ZT6 | 30°C | 3.135984 | 0.27841 | 60 |
| attP40 Control | ZT12 | 25°C | 2.078545 | 0.154971 | 60 |
| attP40 Control | ZT12 | 30°C | 2.870796 | 0.191674 | 60 |
| attP40 Control | ZT18 | 25°C | 1.760688 | 0.114897 | 60 |
| attP40 Control | ZT18 | 30°C | 2.856223 | 0.321228 | 60 |

## Holm-Sidak Pairwise Contrasts Across All Factors: Power Gain

N.b. the first table contains only estimates and standard errors; see second table for T-ratios and p-values.

| Contrast | Estimate | Standard Error |
|---|---|---|
| Naam RNAi 25°C ZT0 - attP40 Control 25°C ZT0 | -2.50804 | 0.638225 |
| Naam RNAi 25°C ZT0 - Naam RNAi 30°C ZT0 | -0.95065 | 0.635668 |
| Naam RNAi 25°C ZT0 - attP40 Control 30°C ZT0 | -3.70975 | 0.635668 |
| Naam RNAi 25°C ZT0 - Naam RNAi 25°C ZT6 | -0.44335 | 0.640857 |
| Naam RNAi 25°C ZT0 - attP40 Control 25°C ZT6 | -2.52745 | 0.640857 |
| Naam RNAi 25°C ZT0 - Naam RNAi 30°C ZT6 | -1.83485 | 0.640857 |
| Naam RNAi 25°C ZT0 - attP40 Control 30°C ZT6 | -5.54649 | 0.640857 |
| Naam RNAi 25°C ZT0 - Naam RNAi 25°C ZT12 | -0.07424 | 0.640857 |
| Naam RNAi 25°C ZT0 - attP40 Control 25°C ZT12 | -2.97802 | 0.640857 |
| Naam RNAi 25°C ZT0 - Naam RNAi 30°C ZT12 | -2.2814 | 0.640857 |
| Naam RNAi 25°C ZT0 - attP40 Control 30°C ZT12 | -4.97926 | 0.640857 |
| Naam RNAi 25°C ZT0 - Naam RNAi 25°C ZT18 | 0.891473 | 0.649235 |
| Naam RNAi 25°C ZT0 - attP40 Control 25°C ZT18 | -2.62399 | 0.640857 |
| Naam RNAi 25°C ZT0 - Naam RNAi 30°C ZT18 | -0.02069 | 0.640857 |
| Naam RNAi 25°C ZT0 - attP40 Control 30°C ZT18 | -4.38353 | 0.640857 |
| attP40 Control 25°C ZT0 - Naam RNAi 30°C ZT0 | 1.557395 | 0.633014 |
| attP40 Control 25°C ZT0 - attP40 Control 30°C ZT0 | -1.2017 | 0.633014 |
| attP40 Control 25°C ZT0 - Naam RNAi 25°C ZT6 | 2.064692 | 0.638225 |
| attP40 Control 25°C ZT0 - attP40 Control 25°C ZT6 | -0.01941 | 0.638225 |
| attP40 Control 25°C ZT0 - Naam RNAi 30°C ZT6 | 0.673193 | 0.638225 |
| attP40 Control 25°C ZT0 - attP40 Control 30°C ZT6 | -3.03845 | 0.638225 |
| attP40 Control 25°C ZT0 - Naam RNAi 25°C ZT12 | 2.433807 | 0.638225 |
| attP40 Control 25°C ZT0 - attP40 Control 25°C ZT12 | -0.46997 | 0.638225 |
| attP40 Control 25°C ZT0 - Naam RNAi 30°C ZT12 | 0.226645 | 0.638225 |
| attP40 Control 25°C ZT0 - attP40 Control 30°C ZT12 | -2.47121 | 0.638225 |
| attP40 Control 25°C ZT0 - Naam RNAi 25°C ZT18 | 3.399517 | 0.646637 |
| attP40 Control 25°C ZT0 - attP40 Control 25°C ZT18 | -0.11595 | 0.638225 |
| attP40 Control 25°C ZT0 - Naam RNAi 30°C ZT18 | 2.487353 | 0.638225 |
| attP40 Control 25°C ZT0 - attP40 Control 30°C ZT18 | -1.87549 | 0.638225 |
| Naam RNAi 30°C ZT0 - attP40 Control 30°C ZT0 | -2.7591 | 0.630436 |
| Naam RNAi 30°C ZT0 - Naam RNAi 25°C ZT6 | 0.507297 | 0.635668 |
| Naam RNAi 30°C ZT0 - attP40 Control 25°C ZT6 | -1.5768 | 0.635668 |
| Naam RNAi 30°C ZT0 - Naam RNAi 30°C ZT6 | -0.8842 | 0.635668 |
| Naam RNAi 30°C ZT0 - attP40 Control 30°C ZT6 | -4.59584 | 0.635668 |
| Naam RNAi 30°C ZT0 - Naam RNAi 25°C ZT12 | 0.876412 | 0.635668 |
| Naam RNAi 30°C ZT0 - attP40 Control 25°C ZT12 | -2.02737 | 0.635668 |
| Naam RNAi 30°C ZT0 - Naam RNAi 30°C ZT12 | -1.33075 | 0.635668 |
| Naam RNAi 30°C ZT0 - attP40 Control 30°C ZT12 | -4.02861 | 0.635668 |
| Naam RNAi 30°C ZT0 - Naam RNAi 25°C ZT18 | 1.842121 | 0.644113 |
| Naam RNAi 30°C ZT0 - attP40 Control 25°C ZT18 | -1.67334 | 0.635668 |
| Naam RNAi 30°C ZT0 - Naam RNAi 30°C ZT18 | 0.929958 | 0.635668 |
| Naam RNAi 30°C ZT0 - attP40 Control 30°C ZT18 | -3.43288 | 0.635668 |
| attP40 Control 30°C ZT0 - Naam RNAi 25°C ZT6 | 3.266394 | 0.635668 |
| attP40 Control 30°C ZT0 - attP40 Control 25°C ZT6 | 1.182293 | 0.635668 |
| attP40 Control 30°C ZT0 - Naam RNAi 30°C ZT6 | 1.874896 | 0.635668 |
| attP40 Control 30°C ZT0 - attP40 Control 30°C ZT6 | -1.83674 | 0.635668 |
| attP40 Control 30°C ZT0 - Naam RNAi 25°C ZT12 | 3.63551 | 0.635668 |
| attP40 Control 30°C ZT0 - attP40 Control 25°C ZT12 | 0.731729 | 0.635668 |

| | | |
|---|---|---|
| attP40 Control 30°C ZT0 - Naam RNAi 30°C ZT12 | 1.428347 | 0.635668 |
| attP40 Control 30°C ZT0 - attP40 Control 30°C ZT12 | -1.26951 | 0.635668 |
| attP40 Control 30°C ZT0 - Naam RNAi 25°C ZT18 | 4.601219 | 0.644113 |
| attP40 Control 30°C ZT0 - attP40 Control 25°C ZT18 | 1.085756 | 0.635668 |
| attP40 Control 30°C ZT0 - Naam RNAi 30°C ZT18 | 3.689056 | 0.635668 |
| attP40 Control 30°C ZT0 - attP40 Control 30°C ZT18 | -0.67378 | 0.635668 |
| Naam RNAi 25°C ZT6 - attP40 Control 25°C ZT6 | -2.0841 | 0.640857 |
| Naam RNAi 25°C ZT6 - Naam RNAi 30°C ZT6 | -1.3915 | 0.640857 |
| Naam RNAi 25°C ZT6 - attP40 Control 30°C ZT6 | -5.10314 | 0.640857 |
| Naam RNAi 25°C ZT6 - Naam RNAi 25°C ZT12 | 0.369115 | 0.640857 |
| Naam RNAi 25°C ZT6 - attP40 Control 25°C ZT12 | -2.53467 | 0.640857 |
| Naam RNAi 25°C ZT6 - Naam RNAi 30°C ZT12 | -1.83805 | 0.640857 |
| Naam RNAi 25°C ZT6 - attP40 Control 30°C ZT12 | -4.5359 | 0.640857 |
| Naam RNAi 25°C ZT6 - Naam RNAi 25°C ZT18 | 1.334825 | 0.649235 |
| Naam RNAi 25°C ZT6 - attP40 Control 25°C ZT18 | -2.18064 | 0.640857 |
| Naam RNAi 25°C ZT6 - Naam RNAi 30°C ZT18 | 0.422662 | 0.640857 |
| Naam RNAi 25°C ZT6 - attP40 Control 30°C ZT18 | -3.94018 | 0.640857 |
| attP40 Control 25°C ZT6 - Naam RNAi 30°C ZT6 | 0.692602 | 0.640857 |
| attP40 Control 25°C ZT6 - attP40 Control 30°C ZT6 | -3.01904 | 0.640857 |
| attP40 Control 25°C ZT6 - Naam RNAi 25°C ZT12 | 2.453216 | 0.640857 |
| attP40 Control 25°C ZT6 - attP40 Control 25°C ZT12 | -0.45056 | 0.640857 |
| attP40 Control 25°C ZT6 - Naam RNAi 30°C ZT12 | 0.246054 | 0.640857 |
| attP40 Control 25°C ZT6 - attP40 Control 30°C ZT12 | -2.4518 | 0.640857 |
| attP40 Control 25°C ZT6 - Naam RNAi 25°C ZT18 | 3.418926 | 0.649235 |
| attP40 Control 25°C ZT6 - attP40 Control 25°C ZT18 | -0.09654 | 0.640857 |
| attP40 Control 25°C ZT6 - Naam RNAi 30°C ZT18 | 2.506763 | 0.640857 |
| attP40 Control 25°C ZT6 - attP40 Control 30°C ZT18 | -1.85608 | 0.640857 |
| Naam RNAi 30°C ZT6 - attP40 Control 30°C ZT6 | -3.71164 | 0.640857 |
| Naam RNAi 30°C ZT6 - Naam RNAi 25°C ZT12 | 1.760614 | 0.640857 |
| Naam RNAi 30°C ZT6 - attP40 Control 25°C ZT12 | -1.14317 | 0.640857 |
| Naam RNAi 30°C ZT6 - Naam RNAi 30°C ZT12 | -0.44655 | 0.640857 |
| Naam RNAi 30°C ZT6 - attP40 Control 30°C ZT12 | -3.14441 | 0.640857 |
| Naam RNAi 30°C ZT6 - Naam RNAi 25°C ZT18 | 2.726324 | 0.649235 |
| Naam RNAi 30°C ZT6 - attP40 Control 25°C ZT18 | -0.78914 | 0.640857 |
| Naam RNAi 30°C ZT6 - Naam RNAi 30°C ZT18 | 1.81416 | 0.640857 |
| Naam RNAi 30°C ZT6 - attP40 Control 30°C ZT18 | -2.54868 | 0.640857 |
| attP40 Control 30°C ZT6 - Naam RNAi 25°C ZT12 | 5.472255 | 0.640857 |
| attP40 Control 30°C ZT6 - attP40 Control 25°C ZT12 | 2.568474 | 0.640857 |
| attP40 Control 30°C ZT6 - Naam RNAi 30°C ZT12 | 3.265092 | 0.640857 |
| attP40 Control 30°C ZT6 - attP40 Control 30°C ZT12 | 0.567235 | 0.640857 |
| attP40 Control 30°C ZT6 - Naam RNAi 25°C ZT18 | 6.437964 | 0.649235 |
| attP40 Control 30°C ZT6 - attP40 Control 25°C ZT18 | 2.922501 | 0.640857 |
| attP40 Control 30°C ZT6 - Naam RNAi 30°C ZT18 | 5.525801 | 0.640857 |
| attP40 Control 30°C ZT6 - attP40 Control 30°C ZT18 | 1.162961 | 0.640857 |
| Naam RNAi 25°C ZT12 - attP40 Control 25°C ZT12 | -2.90378 | 0.640857 |
| Naam RNAi 25°C ZT12 - Naam RNAi 30°C ZT12 | -2.20716 | 0.640857 |
| Naam RNAi 25°C ZT12 - attP40 Control 30°C ZT12 | -4.90502 | 0.640857 |
| Naam RNAi 25°C ZT12 - Naam RNAi 25°C ZT18 | 0.965709 | 0.649235 |
| Naam RNAi 25°C ZT12 - attP40 Control 25°C ZT18 | -2.54975 | 0.640857 |
| Naam RNAi 25°C ZT12 - Naam RNAi 30°C ZT18 | 0.053546 | 0.640857 |
| Naam RNAi 25°C ZT12 - attP40 Control 30°C ZT18 | -4.30929 | 0.640857 |
| attP40 Control 25°C ZT12 - Naam RNAi 30°C ZT12 | 0.696618 | 0.640857 |
| attP40 Control 25°C ZT12 - attP40 Control 30°C ZT12 | -2.00124 | 0.640857 |
| attP40 Control 25°C ZT12 - Naam RNAi 25°C ZT18 | 3.86949 | 0.649235 |
| attP40 Control 25°C ZT12 - attP40 Control 25°C ZT18 | 0.354027 | 0.640857 |
| attP40 Control 25°C ZT12 - Naam RNAi 30°C ZT18 | 2.957327 | 0.640857 |
| attP40 Control 25°C ZT12 - attP40 Control 30°C ZT18 | -1.40551 | 0.640857 |
| Naam RNAi 30°C ZT12 - attP40 Control 30°C ZT12 | -2.69786 | 0.640857 |
| Naam RNAi 30°C ZT12 - Naam RNAi 25°C ZT18 | 3.172872 | 0.649235 |
| Naam RNAi 30°C ZT12 - attP40 Control 25°C ZT18 | -0.34259 | 0.640857 |
| Naam RNAi 30°C ZT12 - Naam RNAi 30°C ZT18 | 2.260709 | 0.640857 |
| Naam RNAi 30°C ZT12 - attP40 Control 30°C ZT18 | -2.10213 | 0.640857 |
| attP40 Control 30°C ZT12 - Naam RNAi 25°C ZT18 | 5.870729 | 0.649235 |
| attP40 Control 30°C ZT12 - attP40 Control 25°C ZT18 | 2.355266 | 0.640857 |
| attP40 Control 30°C ZT12 - Naam RNAi 30°C ZT18 | 4.958566 | 0.640857 |
| attP40 Control 30°C ZT12 - attP40 Control 30°C ZT18 | 0.595726 | 0.640857 |
| Naam RNAi 25°C ZT18 - attP40 Control 25°C ZT18 | -3.51546 | 0.649235 |
| Naam RNAi 25°C ZT18 - Naam RNAi 30°C ZT18 | -0.91216 | 0.649235 |
| Naam RNAi 25°C ZT18 - attP40 Control 30°C ZT18 | -5.275 | 0.649235 |
| attP40 Control 25°C ZT18 - Naam RNAi 30°C ZT18 | 2.6033 | 0.640857 |
| attP40 Control 25°C ZT18 - attP40 Control 30°C ZT18 | -1.75954 | 0.640857 |
| Naam RNAi 30°C ZT18 - attP40 Control 30°C ZT18 | -4.36284 | 0.640857 |

| Contrast | T-ratio | p-value |
|---|---|---|
| attP40 Control 25°C ZT0 - attP40 Control 25°C ZT12 | -0.17584 | 1 |
| attP40 Control 25°C ZT0 - attP40 Control 25°C ZT18 | 0.499315 | 1 |

| | | |
|---|---|---|
| attP40 Control 25°C ZT0 - attP40 Control 25°C ZT6 | -0.21007 | 1 |
| attP40 Control 25°C ZT0 - attP40 Control 30°C ZT0 | -2.15298 | 1 |
| attP40 Control 25°C ZT0 - attP40 Control 30°C ZT12 | -2.9913 | 0.153896 |
| attP40 Control 25°C ZT0 - attP40 Control 30°C ZT18 | -1.48486 | 1 |
| attP40 Control 25°C ZT0 - attP40 Control 30°C ZT6 | -2.15602 | 1 |
| attP40 Control 25°C ZT0 - Naam RNAi 25°C ZT0 | 5.558562 | 3.01E-06 |
| attP40 Control 25°C ZT0 - Naam RNAi 25°C ZT12 | 5.415925 | 6.50E-06 |
| attP40 Control 25°C ZT0 - Naam RNAi 25°C ZT18 | 7.366052 | 3.94E-11 |
| attP40 Control 25°C ZT0 - Naam RNAi 25°C ZT6 | 4.568089 | 0.000412 |
| attP40 Control 25°C ZT0 - Naam RNAi 30°C ZT0 | 3.876702 | 0.007358 |
| attP40 Control 25°C ZT0 - Naam RNAi 30°C ZT12 | 2.154287 | 1 |
| attP40 Control 25°C ZT0 - Naam RNAi 30°C ZT18 | 6.131964 | 1.20E-07 |
| attP40 Control 25°C ZT0 - Naam RNAi 30°C ZT6 | 2.293501 | 0.941152 |
| attP40 Control 25°C ZT12 - attP40 Control 25°C ZT18 | 0.672377 | 1 |
| attP40 Control 25°C ZT12 - attP40 Control 25°C ZT6 | -0.03409 | 1 |
| attP40 Control 25°C ZT12 - attP40 Control 30°C ZT0 | -1.96746 | 1 |
| attP40 Control 25°C ZT12 - attP40 Control 30°C ZT12 | -2.80391 | 0.267908 |
| attP40 Control 25°C ZT12 - attP40 Control 30°C ZT18 | -1.30365 | 1 |
| attP40 Control 25°C ZT12 - attP40 Control 30°C ZT6 | -1.97205 | 1 |
| attP40 Control 25°C ZT12 - Naam RNAi 25°C ZT0 | 5.710847 | 1.34E-06 |
| attP40 Control 25°C ZT12 - Naam RNAi 25°C ZT12 | 5.568796 | 2.87E-06 |
| attP40 Control 25°C ZT12 - Naam RNAi 25°C ZT18 | 7.509432 | 1.43E-11 |
| attP40 Control 25°C ZT12 - Naam RNAi 25°C ZT6 | 4.724442 | 0.000199 |
| attP40 Control 25°C ZT12 - Naam RNAi 30°C ZT0 | 4.037062 | 0.00392 |
| attP40 Control 25°C ZT12 - Naam RNAi 30°C ZT12 | 2.320553 | 0.903007 |
| attP40 Control 25°C ZT12 - Naam RNAi 30°C ZT18 | 6.281894 | 4.84E-08 |
| attP40 Control 25°C ZT12 - Naam RNAi 30°C ZT6 | 2.459195 | 0.66284 |
| attP40 Control 25°C ZT18 - attP40 Control 25°C ZT6 | -0.70647 | 1 |
| attP40 Control 25°C ZT18 - attP40 Control 30°C ZT0 | -2.64532 | 0.414834 |
| attP40 Control 25°C ZT18 - attP40 Control 30°C ZT12 | -3.47628 | 0.031892 |
| attP40 Control 25°C ZT18 - attP40 Control 30°C ZT18 | -1.97603 | 1 |
| attP40 Control 25°C ZT18 - attP40 Control 30°C ZT6 | -2.64443 | 0.414834 |
| attP40 Control 25°C ZT18 - Naam RNAi 25°C ZT0 | 5.038471 | 4.38E-05 |
| attP40 Control 25°C ZT18 - Naam RNAi 25°C ZT12 | 4.896419 | 8.83E-05 |
| attP40 Control 25°C ZT18 - Naam RNAi 25°C ZT18 | 6.845731 | 1.35E-09 |
| attP40 Control 25°C ZT18 - Naam RNAi 25°C ZT6 | 4.052065 | 0.003735 |
| attP40 Control 25°C ZT18 - Naam RNAi 30°C ZT0 | 3.359196 | 0.047149 |
| attP40 Control 25°C ZT18 - Naam RNAi 30°C ZT12 | 1.648176 | 1 |
| attP40 Control 25°C ZT18 - Naam RNAi 30°C ZT18 | 5.609517 | 2.34E-06 |
| attP40 Control 25°C ZT18 - Naam RNAi 30°C ZT6 | 1.786818 | 1 |
| attP40 Control 25°C ZT6 - attP40 Control 30°C ZT0 | -1.93308 | 1 |
| attP40 Control 25°C ZT6 - attP40 Control 30°C ZT12 | -2.76981 | 0.29165 |
| attP40 Control 25°C ZT6 - attP40 Control 30°C ZT18 | -1.26956 | 1 |
| attP40 Control 25°C ZT6 - attP40 Control 30°C ZT6 | -1.93796 | 1 |
| attP40 Control 25°C ZT6 - Naam RNAi 25°C ZT0 | 5.74494 | 1.12E-06 |
| attP40 Control 25°C ZT6 - Naam RNAi 25°C ZT12 | 5.602888 | 2.40E-06 |
| attP40 Control 25°C ZT6 - Naam RNAi 25°C ZT18 | 7.543084 | 1.15E-11 |
| attP40 Control 25°C ZT6 - Naam RNAi 25°C ZT6 | 4.758534 | 0.000171 |
| attP40 Control 25°C ZT6 - Naam RNAi 30°C ZT0 | 4.071433 | 0.003494 |
| attP40 Control 25°C ZT6 - Naam RNAi 30°C ZT12 | 2.354645 | 0.843477 |
| attP40 Control 25°C ZT6 - Naam RNAi 30°C ZT18 | 6.315987 | 3.96E-08 |
| attP40 Control 25°C ZT6 - Naam RNAi 30°C ZT6 | 2.493287 | 0.615676 |
| attP40 Control 30°C ZT0 - attP40 Control 30°C ZT12 | -0.85934 | 1 |
| attP40 Control 30°C ZT0 - attP40 Control 30°C ZT18 | 0.65316 | 1 |
| attP40 Control 30°C ZT0 - attP40 Control 30°C ZT6 | -0.0207 | 1 |
| attP40 Control 30°C ZT0 - Naam RNAi 25°C ZT0 | 7.724923 | 3.16E-12 |
| attP40 Control 30°C ZT0 - Naam RNAi 25°C ZT12 | 7.581712 | 8.78E-12 |
| attP40 Control 30°C ZT0 - Naam RNAi 25°C ZT18 | 9.510803 | 1.80E-18 |
| attP40 Control 30°C ZT0 - Naam RNAi 25°C ZT6 | 6.730465 | 2.87E-09 |
| attP40 Control 30°C ZT0 - Naam RNAi 30°C ZT0 | 6.054348 | 1.89E-07 |
| attP40 Control 30°C ZT0 - Naam RNAi 30°C ZT12 | 4.306952 | 0.001298 |
| attP40 Control 30°C ZT0 - Naam RNAi 30°C ZT18 | 8.300631 | 4.01E-14 |
| attP40 Control 30°C ZT0 - Naam RNAi 30°C ZT6 | 4.446726 | 0.000712 |
| attP40 Control 30°C ZT12 - attP40 Control 30°C ZT18 | 1.500253 | 1 |
| attP40 Control 30°C ZT12 - attP40 Control 30°C ZT6 | 0.831853 | 1 |
| attP40 Control 30°C ZT12 - Naam RNAi 25°C ZT0 | 8.514754 | 7.47E-15 |
| attP40 Control 30°C ZT12 - Naam RNAi 25°C ZT12 | 8.372702 | 2.29E-14 |
| attP40 Control 30°C ZT12 - Naam RNAi 25°C ZT18 | 10.27716 | 1.76E-21 |
| attP40 Control 30°C ZT12 - Naam RNAi 25°C ZT6 | 7.528348 | 1.26E-11 |
| attP40 Control 30°C ZT12 - Naam RNAi 30°C ZT0 | 6.863858 | 1.21E-09 |
| attP40 Control 30°C ZT12 - Naam RNAi 30°C ZT12 | 5.124459 | 2.89E-05 |
| attP40 Control 30°C ZT12 - Naam RNAi 30°C ZT18 | 9.085801 | 6.89E-17 |
| attP40 Control 30°C ZT12 - Naam RNAi 30°C ZT6 | 5.263101 | 1.44E-05 |
| attP40 Control 30°C ZT18 - attP40 Control 30°C ZT6 | -0.6684 | 1 |
| attP40 Control 30°C ZT18 - Naam RNAi 25°C ZT0 | 7.014501 | 4.48E-10 |
| attP40 Control 30°C ZT18 - Naam RNAi 25°C ZT12 | 6.87245 | 1.16E-09 |
| attP40 Control 30°C ZT18 - Naam RNAi 25°C ZT18 | 8.796263 | 7.65E-16 |

| | | |
|---|---|---|
| attP40 Control 30°C ZT18 - Naam RNAi 25°C ZT6 | 6.028096 | 2.19E-07 |
| attP40 Control 30°C ZT18 - Naam RNAi 30°C ZT0 | 5.351358 | 9.09E-06 |
| attP40 Control 30°C ZT18 - Naam RNAi 30°C ZT12 | 3.624206 | 0.018928 |
| attP40 Control 30°C ZT18 - Naam RNAi 30°C ZT18 | 7.585548 | 8.62E-12 |
| attP40 Control 30°C ZT18 - Naam RNAi 30°C ZT6 | 3.762848 | 0.011235 |
| attP40 Control 30°C ZT6 - Naam RNAi 25°C ZT0 | 7.6829 | 4.27E-12 |
| attP40 Control 30°C ZT6 - Naam RNAi 25°C ZT12 | 7.540849 | 1.16E-11 |
| attP40 Control 30°C ZT6 - Naam RNAi 25°C ZT18 | 9.456038 | 2.88E-18 |
| attP40 Control 30°C ZT6 - Naam RNAi 25°C ZT6 | 6.696495 | 3.55E-09 |
| attP40 Control 30°C ZT6 - Naam RNAi 30°C ZT0 | 6.025214 | 2.20E-07 |
| attP40 Control 30°C ZT6 - Naam RNAi 30°C ZT12 | 4.292606 | 0.001363 |
| attP40 Control 30°C ZT6 - Naam RNAi 30°C ZT18 | 8.253947 | 5.73E-14 |
| attP40 Control 30°C ZT6 - Naam RNAi 30°C ZT6 | 4.431248 | 0.000753 |
| Naam RNAi 25°C ZT0 - Naam RNAi 25°C ZT12 | -0.14205 | 1 |
| Naam RNAi 25°C ZT0 - Naam RNAi 25°C ZT18 | 1.872276 | 1 |
| Naam RNAi 25°C ZT0 - Naam RNAi 25°C ZT6 | -0.98641 | 1 |
| Naam RNAi 25°C ZT0 - Naam RNAi 30°C ZT0 | -1.72041 | 1 |
| Naam RNAi 25°C ZT0 - Naam RNAi 30°C ZT12 | -3.39029 | 0.042896 |
| Naam RNAi 25°C ZT0 - Naam RNAi 30°C ZT18 | 0.571047 | 1 |
| Naam RNAi 25°C ZT0 - Naam RNAi 30°C ZT6 | -3.25165 | 0.067711 |
| Naam RNAi 25°C ZT12 - Naam RNAi 25°C ZT18 | 2.012494 | 1 |
| Naam RNAi 25°C ZT12 - Naam RNAi 25°C ZT6 | -0.84435 | 1 |
| Naam RNAi 25°C ZT12 - Naam RNAi 30°C ZT0 | -1.57719 | 1 |
| Naam RNAi 25°C ZT12 - Naam RNAi 30°C ZT12 | -3.24824 | 0.067711 |
| Naam RNAi 25°C ZT12 - Naam RNAi 30°C ZT18 | 0.713098 | 1 |
| Naam RNAi 25°C ZT12 - Naam RNAi 30°C ZT6 | -3.1096 | 0.106121 |
| Naam RNAi 25°C ZT18 - Naam RNAi 25°C ZT6 | -2.84595 | 0.239748 |
| Naam RNAi 25°C ZT18 - Naam RNAi 30°C ZT0 | -3.58501 | 0.021612 |
| Naam RNAi 25°C ZT18 - Naam RNAi 30°C ZT12 | -5.21882 | 1.79E-05 |
| Naam RNAi 25°C ZT18 - Naam RNAi 30°C ZT18 | -1.3086 | 1 |
| Naam RNAi 25°C ZT18 - Naam RNAi 30°C ZT6 | -5.08197 | 3.56E-05 |
| Naam RNAi 25°C ZT6 - Naam RNAi 30°C ZT0 | -0.72595 | 1 |
| Naam RNAi 25°C ZT6 - Naam RNAi 30°C ZT12 | -2.40389 | 0.755005 |
| Naam RNAi 25°C ZT6 - Naam RNAi 30°C ZT18 | 1.557452 | 1 |
| Naam RNAi 25°C ZT6 - Naam RNAi 30°C ZT6 | -2.26525 | 0.97264 |
| Naam RNAi 30°C ZT0 - Naam RNAi 30°C ZT12 | -1.69757 | 1 |
| Naam RNAi 30°C ZT0 - Naam RNAi 30°C ZT18 | 2.296114 | 0.941152 |
| Naam RNAi 30°C ZT0 - Naam RNAi 30°C ZT6 | -1.55779 | 1 |
| Naam RNAi 30°C ZT12 - Naam RNAi 30°C ZT18 | 3.961342 | 0.005288 |
| Naam RNAi 30°C ZT12 - Naam RNAi 30°C ZT6 | 0.138642 | 1 |
| Naam RNAi 30°C ZT18 - Naam RNAi 30°C ZT6 | -3.8227 | 0.009 |

## Holm-Sidak Pairwise Contrasts Across All Factors: Best Frequency

N.b. the first table contains only estimates and standard errors; see second table for T-ratios and p-values.

| Contrast | Estimate | Standard Error |
|---|---|---|
| Naam RNAi 25°C ZT0 - attP40 Control 25°C ZT0 | 28.61549795 | 8.075495447 |
| Naam RNAi 25°C ZT0 - Naam RNAi 30°C ZT0 | -53.85450744 | 8.043137248 |
| Naam RNAi 25°C ZT0 - attP40 Control 30°C ZT0 | -36.85753405 | 8.043137248 |
| Naam RNAi 25°C ZT0 - Naam RNAi 25°C ZT6 | -17.07444271 | 8.1087966 |
| Naam RNAi 25°C ZT0 - attP40 Control 25°C ZT6 | 21.88395788 | 8.1087966 |
| Naam RNAi 25°C ZT0 - Naam RNAi 30°C ZT6 | -56.57815891 | 8.1087966 |
| Naam RNAi 25°C ZT0 - attP40 Control 30°C ZT6 | -33.66303569 | 8.1087966 |
| Naam RNAi 25°C ZT0 - Naam RNAi 25°C ZT12 | -12.59641498 | 8.1087966 |
| Naam RNAi 25°C ZT0 - attP40 Control 25°C ZT12 | 16.71003897 | 8.1087966 |
| Naam RNAi 25°C ZT0 - Naam RNAi 30°C ZT12 | -62.48710686 | 8.1087966 |
| Naam RNAi 25°C ZT0 - attP40 Control 30°C ZT12 | -53.04148624 | 8.1087966 |
| Naam RNAi 25°C ZT0 - Naam RNAi 25°C ZT18 | -57.95972255 | 8.21479844 |
| Naam RNAi 25°C ZT0 - attP40 Control 25°C ZT18 | 17.20777553 | 8.1087966 |
| Naam RNAi 25°C ZT0 - Naam RNAi 30°C ZT18 | -36.78622158 | 8.1087966 |
| Naam RNAi 25°C ZT0 - attP40 Control 30°C ZT18 | -22.33185724 | 8.1087966 |
| attP40 Control 25°C ZT0 - Naam RNAi 30°C ZT0 | -82.47000539 | 8.009563109 |
| attP40 Control 25°C ZT0 - attP40 Control 30°C ZT0 | -65.473032 | 8.009563109 |
| attP40 Control 25°C ZT0 - Naam RNAi 25°C ZT6 | -45.68994067 | 8.075495447 |
| attP40 Control 25°C ZT0 - attP40 Control 25°C ZT6 | -6.731540073 | 8.075495447 |
| attP40 Control 25°C ZT0 - Naam RNAi 30°C ZT6 | -85.19365686 | 8.075495447 |
| attP40 Control 25°C ZT0 - attP40 Control 30°C ZT6 | -62.27853364 | 8.075495447 |
| attP40 Control 25°C ZT0 - Naam RNAi 25°C ZT12 | -41.21191293 | 8.075495447 |
| attP40 Control 25°C ZT0 - attP40 Control 25°C ZT12 | -11.90545898 | 8.075495447 |
| attP40 Control 25°C ZT0 - Naam RNAi 30°C ZT12 | -91.10260482 | 8.075495447 |
| attP40 Control 25°C ZT0 - attP40 Control 30°C ZT12 | -81.65698419 | 8.075495447 |
| attP40 Control 25°C ZT0 - Naam RNAi 25°C ZT18 | -86.5752205 | 8.181928735 |
| attP40 Control 25°C ZT0 - attP40 Control 25°C ZT18 | -11.40772243 | 8.075495447 |
| attP40 Control 25°C ZT0 - Naam RNAi 30°C ZT18 | -65.40171953 | 8.075495447 |

| | | |
|---|---|---|
| attP40 Control 25°C ZT0 - attP40 Control 30°C ZT18 | -50.94735519 | 8.075495447 |
| Naam RNAi 30°C ZT0 - attP40 Control 30°C ZT0 | 16.9969734 | 7.976937461 |
| Naam RNAi 30°C ZT0 - Naam RNAi 25°C ZT6 | 36.78006473 | 8.043137248 |
| Naam RNAi 30°C ZT0 - attP40 Control 25°C ZT6 | 75.73846532 | 8.043137248 |
| Naam RNAi 30°C ZT0 - Naam RNAi 30°C ZT6 | -2.723651465 | 8.043137248 |
| Naam RNAi 30°C ZT0 - attP40 Control 30°C ZT6 | 20.19147175 | 8.043137248 |
| Naam RNAi 30°C ZT0 - Naam RNAi 25°C ZT12 | 41.25809247 | 8.043137248 |
| Naam RNAi 30°C ZT0 - attP40 Control 25°C ZT12 | 70.56454641 | 8.043137248 |
| Naam RNAi 30°C ZT0 - Naam RNAi 30°C ZT12 | -8.632599424 | 8.043137248 |
| Naam RNAi 30°C ZT0 - attP40 Control 30°C ZT12 | 0.8130212 | 8.043137248 |
| Naam RNAi 30°C ZT0 - Naam RNAi 25°C ZT18 | -4.105215109 | 8.149993122 |
| Naam RNAi 30°C ZT0 - attP40 Control 25°C ZT18 | 71.06228297 | 8.043137248 |
| Naam RNAi 30°C ZT0 - Naam RNAi 30°C ZT18 | 17.06828586 | 8.043137248 |
| Naam RNAi 30°C ZT0 - attP40 Control 30°C ZT18 | 31.5226502 | 8.043137248 |
| attP40 Control 30°C ZT0 - Naam RNAi 25°C ZT6 | 19.78309133 | 8.043137248 |
| attP40 Control 30°C ZT0 - attP40 Control 25°C ZT6 | 58.74149193 | 8.043137248 |
| attP40 Control 30°C ZT0 - Naam RNAi 30°C ZT6 | -19.72062486 | 8.043137248 |
| attP40 Control 30°C ZT0 - attP40 Control 30°C ZT6 | 3.194498359 | 8.043137248 |
| attP40 Control 30°C ZT0 - Naam RNAi 25°C ZT12 | 24.26111907 | 8.043137248 |
| attP40 Control 30°C ZT0 - attP40 Control 25°C ZT12 | 53.56757301 | 8.043137248 |
| attP40 Control 30°C ZT0 - Naam RNAi 30°C ZT12 | -25.62957282 | 8.043137248 |
| attP40 Control 30°C ZT0 - attP40 Control 30°C ZT12 | -16.1839522 | 8.043137248 |
| attP40 Control 30°C ZT0 - Naam RNAi 25°C ZT18 | -21.10218851 | 8.149993122 |
| attP40 Control 30°C ZT0 - attP40 Control 25°C ZT18 | 54.06530957 | 8.043137248 |
| attP40 Control 30°C ZT0 - Naam RNAi 30°C ZT18 | 0.071312466 | 8.043137248 |
| attP40 Control 30°C ZT0 - attP40 Control 30°C ZT18 | 14.5256768 | 8.043137248 |
| Naam RNAi 25°C ZT6 - attP40 Control 25°C ZT6 | 38.95840059 | 8.1087966 |
| Naam RNAi 25°C ZT6 - Naam RNAi 30°C ZT6 | -39.50371619 | 8.1087966 |
| Naam RNAi 25°C ZT6 - attP40 Control 30°C ZT6 | -16.58859297 | 8.1087966 |
| Naam RNAi 25°C ZT6 - Naam RNAi 25°C ZT12 | 4.478027736 | 8.1087966 |
| Naam RNAi 25°C ZT6 - attP40 Control 25°C ZT12 | 33.78448168 | 8.1087966 |
| Naam RNAi 25°C ZT6 - Naam RNAi 30°C ZT12 | -45.41266415 | 8.1087966 |
| Naam RNAi 25°C ZT6 - attP40 Control 30°C ZT12 | -35.96704353 | 8.1087966 |
| Naam RNAi 25°C ZT6 - Naam RNAi 25°C ZT18 | -40.88527984 | 8.21479844 |
| Naam RNAi 25°C ZT6 - attP40 Control 25°C ZT18 | 34.28221824 | 8.1087966 |
| Naam RNAi 25°C ZT6 - Naam RNAi 30°C ZT18 | -19.71177887 | 8.1087966 |
| Naam RNAi 25°C ZT6 - attP40 Control 30°C ZT18 | -5.25741453 | 8.1087966 |
| attP40 Control 25°C ZT6 - Naam RNAi 30°C ZT6 | -78.46211679 | 8.1087966 |
| attP40 Control 25°C ZT6 - attP40 Control 30°C ZT6 | -55.54699357 | 8.1087966 |
| attP40 Control 25°C ZT6 - Naam RNAi 25°C ZT12 | -34.48037286 | 8.1087966 |
| attP40 Control 25°C ZT6 - attP40 Control 25°C ZT12 | -5.173918911 | 8.1087966 |
| attP40 Control 25°C ZT6 - Naam RNAi 30°C ZT12 | -84.37106475 | 8.1087966 |
| attP40 Control 25°C ZT6 - attP40 Control 30°C ZT12 | -74.92544412 | 8.1087966 |
| attP40 Control 25°C ZT6 - Naam RNAi 25°C ZT18 | -79.84368043 | 8.21479844 |
| attP40 Control 25°C ZT6 - attP40 Control 25°C ZT18 | -4.676182354 | 8.1087966 |
| attP40 Control 25°C ZT6 - Naam RNAi 30°C ZT18 | -58.67017946 | 8.1087966 |
| attP40 Control 25°C ZT6 - attP40 Control 30°C ZT18 | -44.21581512 | 8.1087966 |
| Naam RNAi 30°C ZT6 - attP40 Control 30°C ZT6 | 22.91512322 | 8.1087966 |
| Naam RNAi 30°C ZT6 - Naam RNAi 25°C ZT12 | 43.98174393 | 8.1087966 |
| Naam RNAi 30°C ZT6 - attP40 Control 25°C ZT12 | 73.28819788 | 8.1087966 |
| Naam RNAi 30°C ZT6 - Naam RNAi 30°C ZT12 | -5.908947959 | 8.1087966 |
| Naam RNAi 30°C ZT6 - attP40 Control 30°C ZT12 | 3.536672665 | 8.1087966 |
| Naam RNAi 30°C ZT6 - Naam RNAi 25°C ZT18 | -1.381563645 | 8.21479844 |
| Naam RNAi 30°C ZT6 - attP40 Control 25°C ZT18 | 73.78593443 | 8.1087966 |
| Naam RNAi 30°C ZT6 - Naam RNAi 30°C ZT18 | 19.79193733 | 8.1087966 |
| Naam RNAi 30°C ZT6 - attP40 Control 30°C ZT18 | 34.24630166 | 8.1087966 |
| attP40 Control 30°C ZT6 - Naam RNAi 25°C ZT12 | 21.06662071 | 8.1087966 |
| attP40 Control 30°C ZT6 - attP40 Control 25°C ZT12 | 50.37307466 | 8.1087966 |
| attP40 Control 30°C ZT6 - Naam RNAi 30°C ZT12 | -28.82407118 | 8.1087966 |
| attP40 Control 30°C ZT6 - attP40 Control 30°C ZT12 | -19.37845055 | 8.1087966 |
| attP40 Control 30°C ZT6 - Naam RNAi 25°C ZT18 | -24.29668686 | 8.21479844 |
| attP40 Control 30°C ZT6 - attP40 Control 25°C ZT18 | 50.87081121 | 8.1087966 |
| attP40 Control 30°C ZT6 - Naam RNAi 30°C ZT18 | -3.123185893 | 8.1087966 |
| attP40 Control 30°C ZT6 - attP40 Control 30°C ZT18 | 11.33117844 | 8.1087966 |
| Naam RNAi 25°C ZT12 - attP40 Control 25°C ZT12 | 29.30645394 | 8.1087966 |
| Naam RNAi 25°C ZT12 - Naam RNAi 30°C ZT12 | -49.89069189 | 8.1087966 |
| Naam RNAi 25°C ZT12 - attP40 Control 30°C ZT12 | -40.44507127 | 8.1087966 |
| Naam RNAi 25°C ZT12 - Naam RNAi 25°C ZT18 | -45.36330758 | 8.21479844 |
| Naam RNAi 25°C ZT12 - attP40 Control 25°C ZT18 | 29.8041905 | 8.1087966 |
| Naam RNAi 25°C ZT12 - Naam RNAi 30°C ZT18 | -24.1898066 | 8.1087966 |
| Naam RNAi 25°C ZT12 - attP40 Control 30°C ZT18 | -9.735442266 | 8.1087966 |
| attP40 Control 25°C ZT12 - Naam RNAi 30°C ZT12 | -79.19714583 | 8.1087966 |
| attP40 Control 25°C ZT12 - attP40 Control 30°C ZT12 | -69.75152521 | 8.1087966 |
| attP40 Control 25°C ZT12 - Naam RNAi 25°C ZT18 | -74.66976152 | 8.21479844 |
| attP40 Control 25°C ZT12 - attP40 Control 25°C ZT18 | 0.497736557 | 8.1087966 |
| attP40 Control 25°C ZT12 - Naam RNAi 30°C ZT18 | -53.49626055 | 8.1087966 |
| attP40 Control 25°C ZT12 - attP40 Control 30°C ZT18 | -39.04189621 | 8.1087966 |

| | | |
|---|---|---|
| Naam RNAi 30°C ZT12 - attP40 Control 30°C ZT12 | 9.445620624 | 8.1087966 |
| Naam RNAi 30°C ZT12 - Naam RNAi 25°C ZT18 | 4.527384314 | 8.21479844 |
| Naam RNAi 30°C ZT12 - attP40 Control 25°C ZT18 | 79.69488239 | 8.1087966 |
| Naam RNAi 30°C ZT12 - Naam RNAi 30°C ZT18 | 25.70088529 | 8.1087966 |
| Naam RNAi 30°C ZT12 - attP40 Control 30°C ZT18 | 40.15524962 | 8.1087966 |
| attP40 Control 30°C ZT12 - Naam RNAi 25°C ZT18 | -4.91823631 | 8.21479844 |
| attP40 Control 30°C ZT12 - attP40 Control 25°C ZT18 | 70.24926177 | 8.1087966 |
| attP40 Control 30°C ZT12 - Naam RNAi 30°C ZT18 | 16.25526466 | 8.1087966 |
| attP40 Control 30°C ZT12 - attP40 Control 30°C ZT18 | 30.709629 | 8.1087966 |
| Naam RNAi 25°C ZT18 - attP40 Control 25°C ZT18 | 75.16749808 | 8.21479844 |
| Naam RNAi 25°C ZT18 - Naam RNAi 30°C ZT18 | 21.17350097 | 8.21479844 |
| Naam RNAi 25°C ZT18 - attP40 Control 30°C ZT18 | 35.62786531 | 8.21479844 |
| attP40 Control 25°C ZT18 - Naam RNAi 30°C ZT18 | -53.99399711 | 8.1087966 |
| attP40 Control 25°C ZT18 - attP40 Control 30°C ZT18 | -39.53963277 | 8.1087966 |
| Naam RNAi 30°C ZT18 - attP40 Control 30°C ZT18 | 14.45436434 | 8.1087966 |

| **Contrast** | **T-ratio** | **p-value** |
|---|---|---|
| attP40 Control 25°C ZT0 - attP40 Control 25°C ZT12 | -2.547278277 | 0.394418633 |
| attP40 Control 25°C ZT0 - attP40 Control 25°C ZT18 | -2.616702356 | 0.335787472 |
| attP40 Control 25°C ZT0 - attP40 Control 25°C ZT6 | -1.70130223 | 1 |
| attP40 Control 25°C ZT0 - attP40 Control 30°C ZT0 | -10.91468619 | 3.78E-24 |
| attP40 Control 25°C ZT0 - attP40 Control 30°C ZT12 | -12.10576833 | 2.13E-29 |
| attP40 Control 25°C ZT0 - attP40 Control 30°C ZT18 | -8.13175947 | 1.20E-13 |
| attP40 Control 25°C ZT0 - attP40 Control 30°C ZT6 | -9.919117708 | 4.11E-20 |
| attP40 Control 25°C ZT0 - Naam RNAi 25°C ZT0 | -4.336922937 | 0.000927978 |
| attP40 Control 25°C ZT0 - Naam RNAi 25°C ZT12 | -6.402601058 | 1.88E-08 |
| attP40 Control 25°C ZT0 - Naam RNAi 25°C ZT18 | -10.18333173 | 3.75E-21 |
| attP40 Control 25°C ZT0 - Naam RNAi 25°C ZT6 | -7.0635848 | 2.61E-10 |
| attP40 Control 25°C ZT0 - Naam RNAi 30°C ZT0 | -12.99630024 | 1.41E-33 |
| attP40 Control 25°C ZT0 - Naam RNAi 30°C ZT12 | -13.35914316 | 2.45E-35 |
| attP40 Control 25°C ZT0 - Naam RNAi 30°C ZT18 | -10.12219353 | 6.54E-21 |
| attP40 Control 25°C ZT0 - Naam RNAi 30°C ZT6 | -12.56263696 | 1.63E-31 |
| attP40 Control 25°C ZT12 - attP40 Control 25°C ZT18 | -0.069138968 | 1 |
| attP40 Control 25°C ZT12 - attP40 Control 25°C ZT6 | 0.842501798 | 1 |
| attP40 Control 25°C ZT12 - attP40 Control 30°C ZT0 | -8.311599279 | 3.09E-14 |
| attP40 Control 25°C ZT12 - attP40 Control 30°C ZT12 | -9.519235304 | 1.43E-18 |
| attP40 Control 25°C ZT12 - attP40 Control 30°C ZT18 | -5.561546882 | 2.47E-06 |
| attP40 Control 25°C ZT12 - attP40 Control 30°C ZT6 | -7.341564808 | 3.86E-11 |
| attP40 Control 25°C ZT12 - Naam RNAi 25°C ZT0 | -1.782294959 | 1 |
| attP40 Control 25°C ZT12 - Naam RNAi 25°C ZT12 | -3.839489767 | 0.007232051 |
| attP40 Control 25°C ZT12 - Naam RNAi 25°C ZT18 | -7.638502734 | 4.78E-12 |
| attP40 Control 25°C ZT12 - Naam RNAi 25°C ZT6 | -4.497758985 | 0.000478635 |
| attP40 Control 25°C ZT12 - Naam RNAi 30°C ZT0 | -10.38452413 | 5.90E-22 |
| attP40 Control 25°C ZT12 - Naam RNAi 30°C ZT12 | -10.76746278 | 1.56E-23 |
| attP40 Control 25°C ZT12 - Naam RNAi 30°C ZT18 | -7.54380664 | 9.31E-12 |
| attP40 Control 25°C ZT12 - Naam RNAi 30°C ZT6 | -9.974227675 | 2.52E-20 |
| attP40 Control 25°C ZT18 - attP40 Control 25°C ZT6 | 0.911640766 | 1 |
| attP40 Control 25°C ZT18 - attP40 Control 30°C ZT0 | -8.241895902 | 5.28E-14 |
| attP40 Control 25°C ZT18 - attP40 Control 30°C ZT12 | -9.450096335 | 2.60E-18 |
| attP40 Control 25°C ZT18 - attP40 Control 30°C ZT18 | -5.492407913 | 3.52E-06 |
| attP40 Control 25°C ZT18 - attP40 Control 30°C ZT6 | -7.27242584 | 6.21E-11 |
| attP40 Control 25°C ZT18 - Naam RNAi 25°C ZT0 | -1.71315599 | 1 |
| attP40 Control 25°C ZT18 - Naam RNAi 25°C ZT12 | -3.770350798 | 0.009025776 |
| attP40 Control 25°C ZT18 - Naam RNAi 25°C ZT18 | -7.570255919 | 7.77E-12 |
| attP40 Control 25°C ZT18 - Naam RNAi 25°C ZT6 | -4.428620017 | 0.000635411 |
| attP40 Control 25°C ZT18 - Naam RNAi 30°C ZT0 | -10.31482076 | 1.11E-21 |
| attP40 Control 25°C ZT18 - Naam RNAi 30°C ZT12 | -10.69832382 | 3.00E-23 |
| attP40 Control 25°C ZT18 - Naam RNAi 30°C ZT18 | -7.474667672 | 1.51E-11 |
| attP40 Control 25°C ZT18 - Naam RNAi 30°C ZT6 | -9.905088707 | 4.63E-20 |
| attP40 Control 25°C ZT6 - attP40 Control 30°C ZT0 | -9.160978757 | 3.11E-17 |
| attP40 Control 25°C ZT6 - attP40 Control 30°C ZT12 | -10.3617371 | 7.24E-22 |
| attP40 Control 25°C ZT6 - attP40 Control 30°C ZT18 | -6.40404868 | 1.88E-08 |
| attP40 Control 25°C ZT6 - attP40 Control 30°C ZT6 | -8.184066606 | 8.11E-14 |
| attP40 Control 25°C ZT6 - Naam RNAi 25°C ZT0 | -2.624796757 | 0.335787472 |
| attP40 Control 25°C ZT6 - Naam RNAi 25°C ZT12 | -4.681991565 | 0.000205125 |
| attP40 Control 25°C ZT6 - Naam RNAi 25°C ZT18 | -8.470133085 | 9.00E-15 |
| attP40 Control 25°C ZT6 - Naam RNAi 25°C ZT6 | -5.340260783 | 7.79E-06 |
| attP40 Control 25°C ZT6 - Naam RNAi 30°C ZT0 | -11.23390361 | 1.63E-25 |
| attP40 Control 25°C ZT6 - Naam RNAi 30°C ZT12 | -11.60996458 | 3.66E-27 |
| attP40 Control 25°C ZT6 - Naam RNAi 30°C ZT18 | -8.386308439 | 1.73E-14 |
| attP40 Control 25°C ZT6 - Naam RNAi 30°C ZT6 | -10.81672947 | 9.74E-24 |
| attP40 Control 30°C ZT0 - attP40 Control 30°C ZT12 | -1.285345357 | 1 |
| attP40 Control 30°C ZT0 - attP40 Control 30°C ZT18 | 2.704651261 | 0.278417108 |
| attP40 Control 30°C ZT0 - attP40 Control 30°C ZT6 | 0.910102335 | 1 |
| attP40 Control 30°C ZT0 - Naam RNAi 25°C ZT0 | 6.514754733 | 9.57E-09 |
| attP40 Control 30°C ZT0 - Naam RNAi 25°C ZT12 | 4.440766219 | 0.000611293 |

| | | |
|---|---|---|
| attP40 Control 30°C ZT0 - Naam RNAi 25°C ZT18 | 0.503383665 | 1 |
| attP40 Control 30°C ZT0 - Naam RNAi 25°C ZT6 | 3.777123285 | 0.009025776 |
| attP40 Control 30°C ZT0 - Naam RNAi 30°C ZT0 | -2.090127845 | 1 |
| attP40 Control 30°C ZT0 - Naam RNAi 30°C ZT12 | -2.543762618 | 0.394418633 |
| attP40 Control 30°C ZT0 - Naam RNAi 30°C ZT18 | 0.706209522 | 1 |
| attP40 Control 30°C ZT0 - Naam RNAi 30°C ZT6 | -1.744052014 | 1 |
| attP40 Control 30°C ZT12 - attP40 Control 30°C ZT18 | 3.957688422 | 0.004636493 |
| attP40 Control 30°C ZT12 - attP40 Control 30°C ZT6 | 2.177670495 | 0.91998817 |
| attP40 Control 30°C ZT12 - Naam RNAi 25°C ZT0 | 7.736940345 | 2.34E-12 |
| attP40 Control 30°C ZT12 - Naam RNAi 25°C ZT12 | 5.679745537 | 1.29E-06 |
| attP40 Control 30°C ZT12 - Naam RNAi 25°C ZT18 | 1.757898581 | 1 |
| attP40 Control 30°C ZT12 - Naam RNAi 25°C ZT6 | 5.021476319 | 3.98E-05 |
| attP40 Control 30°C ZT12 - Naam RNAi 30°C ZT0 | -0.787579497 | 1 |
| attP40 Control 30°C ZT12 - Naam RNAi 30°C ZT12 | -1.24822748 | 1 |
| attP40 Control 30°C ZT12 - Naam RNAi 30°C ZT18 | 1.975428663 | 1 |
| attP40 Control 30°C ZT12 - Naam RNAi 30°C ZT6 | -0.454992372 | 1 |
| attP40 Control 30°C ZT18 - attP40 Control 30°C ZT6 | -1.780017927 | 1 |
| attP40 Control 30°C ZT18 - Naam RNAi 25°C ZT0 | 3.779251923 | 0.009025776 |
| attP40 Control 30°C ZT18 - Naam RNAi 25°C ZT12 | 1.722057115 | 1 |
| attP40 Control 30°C ZT18 - Naam RNAi 25°C ZT18 | -2.148720754 | 0.957293111 |
| attP40 Control 30°C ZT18 - Naam RNAi 25°C ZT6 | 1.063787897 | 1 |
| attP40 Control 30°C ZT18 - Naam RNAi 30°C ZT0 | -4.777576115 | 0.000131561 |
| attP40 Control 30°C ZT18 - Naam RNAi 30°C ZT12 | -5.205915902 | 1.56E-05 |
| attP40 Control 30°C ZT18 - Naam RNAi 30°C ZT18 | -1.982259759 | 1 |
| attP40 Control 30°C ZT18 - Naam RNAi 30°C ZT6 | -4.412680793 | 0.000671649 |
| attP40 Control 30°C ZT6 - Naam RNAi 25°C ZT0 | 5.55926985 | 2.47E-06 |
| attP40 Control 30°C ZT6 - Naam RNAi 25°C ZT12 | 3.502075042 | 0.024161703 |
| attP40 Control 30°C ZT6 - Naam RNAi 25°C ZT18 | -0.391671763 | 1 |
| attP40 Control 30°C ZT6 - Naam RNAi 25°C ZT6 | 2.843805824 | 0.19581624 |
| attP40 Control 30°C ZT6 - Naam RNAi 30°C ZT0 | -2.983027189 | 0.128804875 |
| attP40 Control 30°C ZT6 - Naam RNAi 30°C ZT12 | -3.425897975 | 0.031317363 |
| attP40 Control 30°C ZT6 - Naam RNAi 30°C ZT18 | -0.202241832 | 1 |
| attP40 Control 30°C ZT6 - Naam RNAi 30°C ZT6 | -2.632662867 | 0.335787472 |
| Naam RNAi 25°C ZT0 - Naam RNAi 25°C ZT12 | -2.057194808 | 1 |
| Naam RNAi 25°C ZT0 - Naam RNAi 25°C ZT18 | -5.879206093 | 4.28E-07 |
| Naam RNAi 25°C ZT0 - Naam RNAi 25°C ZT6 | -2.715464026 | 0.276294733 |
| Naam RNAi 25°C ZT0 - Naam RNAi 30°C ZT0 | -8.587679587 | 3.54E-15 |
| Naam RNAi 25°C ZT0 - Naam RNAi 30°C ZT12 | -8.985167825 | 1.36E-16 |
| Naam RNAi 25°C ZT0 - Naam RNAi 30°C ZT18 | -5.761511682 | 8.23E-07 |
| Naam RNAi 25°C ZT0 - Naam RNAi 30°C ZT6 | -8.191932717 | 7.71E-14 |
| Naam RNAi 25°C ZT12 - Naam RNAi 25°C ZT18 | -3.848556846 | 0.00710036 |
| Naam RNAi 25°C ZT12 - Naam RNAi 25°C ZT6 | -0.658269218 | 1 |
| Naam RNAi 25°C ZT12 - Naam RNAi 30°C ZT0 | -6.513691073 | 9.57E-09 |
| Naam RNAi 25°C ZT12 - Naam RNAi 30°C ZT12 | -6.927973017 | 6.47E-10 |
| Naam RNAi 25°C ZT12 - Naam RNAi 30°C ZT18 | -3.704316874 | 0.011436315 |
| Naam RNAi 25°C ZT12 - Naam RNAi 30°C ZT6 | -6.134737908 | 9.52E-08 |
| Naam RNAi 25°C ZT18 - Naam RNAi 25°C ZT6 | 3.19878178 | 0.067021049 |
| Naam RNAi 25°C ZT18 - Naam RNAi 30°C ZT0 | -2.549130066 | 0.394418633 |
| Naam RNAi 25°C ZT18 - Naam RNAi 30°C ZT12 | -2.990019225 | 0.128781877 |
| Naam RNAi 25°C ZT18 - Naam RNAi 30°C ZT18 | 0.192039612 | 1 |
| Naam RNAi 25°C ZT18 - Naam RNAi 30°C ZT6 | -2.207019837 | 0.881669272 |
| Naam RNAi 25°C ZT6 - Naam RNAi 30°C ZT0 | -5.850048139 | 5.01E-07 |
| Naam RNAi 25°C ZT6 - Naam RNAi 30°C ZT12 | -6.269703798 | 4.23E-08 |
| Naam RNAi 25°C ZT6 - Naam RNAi 30°C ZT18 | -3.046047656 | 0.109617773 |
| Naam RNAi 25°C ZT6 - Naam RNAi 30°C ZT6 | -5.47646869 | 3.78E-06 |
| Naam RNAi 30°C ZT0 - Naam RNAi 30°C ZT12 | -0.470837764 | 1 |
| Naam RNAi 30°C ZT0 - Naam RNAi 30°C ZT18 | 2.779134376 | 0.233453005 |
| Naam RNAi 30°C ZT0 - Naam RNAi 30°C ZT6 | 0.32887284 | 1 |
| Naam RNAi 30°C ZT12 - Naam RNAi 30°C ZT18 | 3.223656143 | 0.062830391 |
| Naam RNAi 30°C ZT12 - Naam RNAi 30°C ZT6 | 0.793235108 | 1 |
| Naam RNAi 30°C ZT18 - Naam RNAi 30°C ZT6 | -2.430421035 | 0.503788342 |

## Holm-Sidak Pairwise Contrasts Across All Factors: Tuning Sharpness

N.b. the first table contains only estimates and standard errors; see second table for T-ratios and p-values.

| Contrast | Estimate | Standard Error |
|---|---|---|
| Naam RNAi 25°C ZT0 - attP40 Control 25°C ZT0 | -0.182164829 | 0.245445546 |
| Naam RNAi 25°C ZT0 - Naam RNAi 30°C ZT0 | -0.634928958 | 0.244462055 |
| Naam RNAi 25°C ZT0 - attP40 Control 30°C ZT0 | -0.938060331 | 0.244462055 |
| Naam RNAi 25°C ZT0 - Naam RNAi 25°C ZT6 | -0.140191531 | 0.246457696 |
| Naam RNAi 25°C ZT0 - attP40 Control 25°C ZT6 | -0.034246708 | 0.246457696 |
| Naam RNAi 25°C ZT0 - Naam RNAi 30°C ZT6 | -0.867879668 | 0.246457696 |
| Naam RNAi 25°C ZT0 - attP40 Control 30°C ZT6 | -1.598734356 | 0.246457696 |
| Naam RNAi 25°C ZT0 - Naam RNAi 25°C ZT12 | -0.248767313 | 0.246457696 |

| | | |
|---|---|---|
| Naam RNAi 25°C ZT0 - attP40 Control 25°C ZT12 | -0.541295529 | 0.246457696 |
| Naam RNAi 25°C ZT0 - Naam RNAi 30°C ZT12 | -1.078345119 | 0.246457696 |
| Naam RNAi 25°C ZT0 - attP40 Control 30°C ZT12 | -1.33354605 | 0.246457696 |
| Naam RNAi 25°C ZT0 - Naam RNAi 25°C ZT18 | -0.23002784 | 0.249679502 |
| Naam RNAi 25°C ZT0 - attP40 Control 25°C ZT18 | -0.22343845 | 0.246457696 |
| Naam RNAi 25°C ZT0 - Naam RNAi 30°C ZT18 | -0.39969532 | 0.246457696 |
| Naam RNAi 25°C ZT0 - attP40 Control 30°C ZT18 | -1.318973074 | 0.246457696 |
| attP40 Control 25°C ZT0 - Naam RNAi 30°C ZT0 | -0.452764129 | 0.243441607 |
| attP40 Control 25°C ZT0 - attP40 Control 30°C ZT0 | -0.755895501 | 0.243441607 |
| attP40 Control 25°C ZT0 - Naam RNAi 25°C ZT6 | 0.041973298 | 0.245445546 |
| attP40 Control 25°C ZT0 - attP40 Control 25°C ZT6 | 0.147918121 | 0.245445546 |
| attP40 Control 25°C ZT0 - Naam RNAi 30°C ZT6 | -0.685714839 | 0.245445546 |
| attP40 Control 25°C ZT0 - attP40 Control 30°C ZT6 | -1.416569526 | 0.245445546 |
| attP40 Control 25°C ZT0 - Naam RNAi 25°C ZT12 | -0.066602484 | 0.245445546 |
| attP40 Control 25°C ZT0 - attP40 Control 25°C ZT12 | -0.3591307 | 0.245445546 |
| attP40 Control 25°C ZT0 - Naam RNAi 30°C ZT12 | -0.896180289 | 0.245445546 |
| attP40 Control 25°C ZT0 - attP40 Control 30°C ZT12 | -1.151381221 | 0.245445546 |
| attP40 Control 25°C ZT0 - Naam RNAi 25°C ZT18 | -0.04786301 | 0.248680465 |
| attP40 Control 25°C ZT0 - attP40 Control 25°C ZT18 | -0.041273621 | 0.245445546 |
| attP40 Control 25°C ZT0 - Naam RNAi 30°C ZT18 | -0.217530491 | 0.245445546 |
| attP40 Control 25°C ZT0 - attP40 Control 30°C ZT18 | -1.136808245 | 0.245445546 |
| Naam RNAi 30°C ZT0 - attP40 Control 30°C ZT0 | -0.303131373 | 0.242449987 |
| Naam RNAi 30°C ZT0 - Naam RNAi 25°C ZT6 | 0.494737427 | 0.244462055 |
| Naam RNAi 30°C ZT0 - attP40 Control 25°C ZT6 | 0.60068225 | 0.244462055 |
| Naam RNAi 30°C ZT0 - Naam RNAi 30°C ZT6 | -0.23295071 | 0.244462055 |
| Naam RNAi 30°C ZT0 - attP40 Control 30°C ZT6 | -0.963805398 | 0.244462055 |
| Naam RNAi 30°C ZT0 - Naam RNAi 25°C ZT12 | 0.386161645 | 0.244462055 |
| Naam RNAi 30°C ZT0 - attP40 Control 25°C ZT12 | 0.093633429 | 0.244462055 |
| Naam RNAi 30°C ZT0 - Naam RNAi 30°C ZT12 | -0.443416161 | 0.244462055 |
| Naam RNAi 30°C ZT0 - attP40 Control 30°C ZT12 | -0.698617092 | 0.244462055 |
| Naam RNAi 30°C ZT0 - Naam RNAi 25°C ZT18 | 0.404901118 | 0.247709818 |
| Naam RNAi 30°C ZT0 - attP40 Control 25°C ZT18 | 0.411490508 | 0.244462055 |
| Naam RNAi 30°C ZT0 - Naam RNAi 30°C ZT18 | 0.235233638 | 0.244462055 |
| Naam RNAi 30°C ZT0 - attP40 Control 30°C ZT18 | -0.684044116 | 0.244462055 |
| attP40 Control 30°C ZT0 - Naam RNAi 25°C ZT6 | 0.7978688 | 0.244462055 |
| attP40 Control 30°C ZT0 - attP40 Control 25°C ZT6 | 0.903813622 | 0.244462055 |
| attP40 Control 30°C ZT0 - Naam RNAi 30°C ZT6 | 0.070180662 | 0.244462055 |
| attP40 Control 30°C ZT0 - attP40 Control 30°C ZT6 | -0.660674025 | 0.244462055 |
| attP40 Control 30°C ZT0 - Naam RNAi 25°C ZT12 | 0.689293017 | 0.244462055 |
| attP40 Control 30°C ZT0 - attP40 Control 25°C ZT12 | 0.396764802 | 0.244462055 |
| attP40 Control 30°C ZT0 - Naam RNAi 30°C ZT12 | -0.140284788 | 0.244462055 |
| attP40 Control 30°C ZT0 - attP40 Control 30°C ZT12 | -0.395485719 | 0.244462055 |
| attP40 Control 30°C ZT0 - Naam RNAi 25°C ZT18 | 0.708032491 | 0.247709818 |
| attP40 Control 30°C ZT0 - attP40 Control 25°C ZT18 | 0.71462188 | 0.244462055 |
| attP40 Control 30°C ZT0 - Naam RNAi 30°C ZT18 | 0.53836501 | 0.244462055 |
| attP40 Control 30°C ZT0 - attP40 Control 30°C ZT18 | -0.380912744 | 0.244462055 |
| Naam RNAi 25°C ZT6 - attP40 Control 25°C ZT6 | 0.105944823 | 0.246457696 |
| Naam RNAi 25°C ZT6 - Naam RNAi 30°C ZT6 | -0.727688137 | 0.246457696 |
| Naam RNAi 25°C ZT6 - attP40 Control 30°C ZT6 | -1.458542825 | 0.246457696 |
| Naam RNAi 25°C ZT6 - Naam RNAi 25°C ZT12 | -0.108575783 | 0.246457696 |
| Naam RNAi 25°C ZT6 - attP40 Control 25°C ZT12 | -0.401103998 | 0.246457696 |
| Naam RNAi 25°C ZT6 - Naam RNAi 30°C ZT12 | -0.938153588 | 0.246457696 |
| Naam RNAi 25°C ZT6 - attP40 Control 30°C ZT12 | -1.193354519 | 0.246457696 |
| Naam RNAi 25°C ZT6 - Naam RNAi 25°C ZT18 | -0.089836309 | 0.249679502 |
| Naam RNAi 25°C ZT6 - attP40 Control 25°C ZT18 | -0.083246919 | 0.246457696 |
| Naam RNAi 25°C ZT6 - Naam RNAi 30°C ZT18 | -0.259503789 | 0.246457696 |
| Naam RNAi 25°C ZT6 - attP40 Control 30°C ZT18 | -1.178781543 | 0.246457696 |
| attP40 Control 25°C ZT6 - Naam RNAi 30°C ZT6 | -0.83363296 | 0.246457696 |
| attP40 Control 25°C ZT6 - attP40 Control 30°C ZT6 | -1.564487647 | 0.246457696 |
| attP40 Control 25°C ZT6 - Naam RNAi 25°C ZT12 | -0.214520605 | 0.246457696 |
| attP40 Control 25°C ZT6 - attP40 Control 25°C ZT12 | -0.507048821 | 0.246457696 |
| attP40 Control 25°C ZT6 - Naam RNAi 30°C ZT12 | -1.04409841 | 0.246457696 |
| attP40 Control 25°C ZT6 - attP40 Control 30°C ZT12 | -1.299299342 | 0.246457696 |
| attP40 Control 25°C ZT6 - Naam RNAi 25°C ZT18 | -0.195781132 | 0.249679502 |
| attP40 Control 25°C ZT6 - attP40 Control 25°C ZT18 | -0.189191742 | 0.246457696 |
| attP40 Control 25°C ZT6 - Naam RNAi 30°C ZT18 | -0.365448612 | 0.246457696 |
| attP40 Control 25°C ZT6 - attP40 Control 30°C ZT18 | -1.284726366 | 0.246457696 |
| Naam RNAi 30°C ZT6 - attP40 Control 30°C ZT6 | -0.730854687 | 0.246457696 |
| Naam RNAi 30°C ZT6 - Naam RNAi 25°C ZT12 | 0.619112355 | 0.246457696 |
| Naam RNAi 30°C ZT6 - attP40 Control 25°C ZT12 | 0.326584139 | 0.246457696 |
| Naam RNAi 30°C ZT6 - Naam RNAi 30°C ZT12 | -0.21046545 | 0.246457696 |
| Naam RNAi 30°C ZT6 - attP40 Control 30°C ZT12 | -0.465666382 | 0.246457696 |
| Naam RNAi 30°C ZT6 - Naam RNAi 25°C ZT18 | 0.637851829 | 0.249679502 |
| Naam RNAi 30°C ZT6 - attP40 Control 25°C ZT18 | 0.644441218 | 0.246457696 |
| Naam RNAi 30°C ZT6 - Naam RNAi 30°C ZT18 | 0.468184348 | 0.246457696 |
| Naam RNAi 30°C ZT6 - attP40 Control 30°C ZT18 | -0.451093406 | 0.246457696 |
| attP40 Control 30°C ZT6 - Naam RNAi 25°C ZT12 | 1.349967042 | 0.246457696 |

| | | |
|---|---|---|
| attP40 Control 30°C ZT6 - attP40 Control 25°C ZT12 | 1.057438827 | 0.246457696 |
| attP40 Control 30°C ZT6 - Naam RNAi 30°C ZT12 | 0.520389237 | 0.246457696 |
| attP40 Control 30°C ZT6 - attP40 Control 30°C ZT12 | 0.265188306 | 0.246457696 |
| attP40 Control 30°C ZT6 - Naam RNAi 25°C ZT18 | 1.368706516 | 0.249679502 |
| attP40 Control 30°C ZT6 - attP40 Control 25°C ZT18 | 1.375295905 | 0.246457696 |
| attP40 Control 30°C ZT6 - Naam RNAi 30°C ZT18 | 1.199039035 | 0.246457696 |
| attP40 Control 30°C ZT6 - attP40 Control 30°C ZT18 | 0.279761281 | 0.246457696 |
| Naam RNAi 25°C ZT12 - attP40 Control 25°C ZT12 | -0.292528216 | 0.246457696 |
| Naam RNAi 25°C ZT12 - Naam RNAi 30°C ZT12 | -0.829577805 | 0.246457696 |
| Naam RNAi 25°C ZT12 - attP40 Control 30°C ZT12 | -1.084778736 | 0.246457696 |
| Naam RNAi 25°C ZT12 - Naam RNAi 25°C ZT18 | 0.018739474 | 0.249679502 |
| Naam RNAi 25°C ZT12 - attP40 Control 25°C ZT18 | 0.025328863 | 0.246457696 |
| Naam RNAi 25°C ZT12 - Naam RNAi 30°C ZT18 | -0.150928007 | 0.246457696 |
| Naam RNAi 25°C ZT12 - attP40 Control 30°C ZT18 | -1.070205761 | 0.246457696 |
| attP40 Control 25°C ZT12 - Naam RNAi 30°C ZT12 | -0.537049589 | 0.246457696 |
| attP40 Control 25°C ZT12 - attP40 Control 30°C ZT12 | -0.792250521 | 0.246457696 |
| attP40 Control 25°C ZT12 - Naam RNAi 25°C ZT18 | 0.311267689 | 0.249679502 |
| attP40 Control 25°C ZT12 - attP40 Control 25°C ZT18 | 0.317857079 | 0.246457696 |
| attP40 Control 25°C ZT12 - Naam RNAi 30°C ZT18 | 0.141600209 | 0.246457696 |
| attP40 Control 25°C ZT12 - attP40 Control 30°C ZT18 | -0.777677545 | 0.246457696 |
| Naam RNAi 30°C ZT12 - attP40 Control 30°C ZT12 | -0.255200931 | 0.246457696 |
| Naam RNAi 30°C ZT12 - Naam RNAi 25°C ZT18 | 0.848317279 | 0.249679502 |
| Naam RNAi 30°C ZT12 - attP40 Control 25°C ZT18 | 0.854906668 | 0.246457696 |
| Naam RNAi 30°C ZT12 - Naam RNAi 30°C ZT18 | 0.678649798 | 0.246457696 |
| Naam RNAi 30°C ZT12 - attP40 Control 30°C ZT18 | -0.240627956 | 0.246457696 |
| attP40 Control 30°C ZT12 - Naam RNAi 25°C ZT18 | 1.10351821 | 0.249679502 |
| attP40 Control 30°C ZT12 - attP40 Control 25°C ZT18 | 1.1101076 | 0.246457696 |
| attP40 Control 30°C ZT12 - Naam RNAi 30°C ZT18 | 0.93385073 | 0.246457696 |
| attP40 Control 30°C ZT12 - attP40 Control 30°C ZT18 | 0.014572976 | 0.246457696 |
| Naam RNAi 25°C ZT18 - attP40 Control 25°C ZT18 | 0.006589389 | 0.249679502 |
| Naam RNAi 25°C ZT18 - Naam RNAi 30°C ZT18 | -0.16966748 | 0.249679502 |
| Naam RNAi 25°C ZT18 - attP40 Control 30°C ZT18 | -1.088945235 | 0.249679502 |
| attP40 Control 25°C ZT18 - Naam RNAi 30°C ZT18 | -0.17625687 | 0.246457696 |
| attP40 Control 25°C ZT18 - attP40 Control 30°C ZT18 | -1.095534624 | 0.246457696 |
| Naam RNAi 30°C ZT18 - attP40 Control 30°C ZT18 | -0.919277754 | 0.246457696 |

| **Contrast** | **T-ratio** | **p-value** |
|---|---|---|
| attP40 Control 25°C ZT0 - attP40 Control 25°C ZT12 | -1.473998687 | 1 |
| attP40 Control 25°C ZT0 - attP40 Control 25°C ZT18 | 0.301506922 | 1 |
| attP40 Control 25°C ZT0 - attP40 Control 25°C ZT6 | 1.233471921 | 1 |
| attP40 Control 25°C ZT0 - attP40 Control 30°C ZT0 | -4.757787825 | 0.000233037 |
| attP40 Control 25°C ZT0 - attP40 Control 30°C ZT12 | -5.748896876 | 1.39E-06 |
| attP40 Control 25°C ZT0 - attP40 Control 30°C ZT18 | -4.520254013 | 0.000709809 |
| attP40 Control 25°C ZT0 - attP40 Control 30°C ZT6 | -4.953077366 | 9.17E-05 |
| attP40 Control 25°C ZT0 - Naam RNAi 25°C ZT0 | 0.477303031 | 1 |
| attP40 Control 25°C ZT0 - Naam RNAi 25°C ZT12 | -0.884502754 | 1 |
| attP40 Control 25°C ZT0 - Naam RNAi 25°C ZT18 | -0.429790785 | 1 |
| attP40 Control 25°C ZT0 - Naam RNAi 25°C ZT6 | -0.532208755 | 1 |
| attP40 Control 25°C ZT0 - Naam RNAi 30°C ZT0 | -2.826839971 | 0.344452774 |
| attP40 Control 25°C ZT0 - Naam RNAi 30°C ZT12 | -3.086340243 | 0.162657016 |
| attP40 Control 25°C ZT0 - Naam RNAi 30°C ZT18 | -1.606108937 | 1 |
| attP40 Control 25°C ZT0 - Naam RNAi 30°C ZT6 | -2.669833295 | 0.5326099 |
| attP40 Control 25°C ZT12 - attP40 Control 25°C ZT18 | 1.768213974 | 1 |
| attP40 Control 25°C ZT12 - attP40 Control 25°C ZT6 | 2.696351586 | 0.499442479 |
| attP40 Control 25°C ZT12 - attP40 Control 30°C ZT0 | -3.257998881 | 0.095280623 |
| attP40 Control 25°C ZT12 - attP40 Control 30°C ZT12 | -4.257342065 | 0.002229454 |
| attP40 Control 25°C ZT12 - attP40 Control 30°C ZT18 | -3.033744984 | 0.188583055 |
| attP40 Control 25°C ZT12 - attP40 Control 30°C ZT6 | -3.464790821 | 0.047684174 |
| attP40 Control 25°C ZT12 - Naam RNAi 25°C ZT0 | 1.943288125 | 1 |
| attP40 Control 25°C ZT12 - Naam RNAi 25°C ZT12 | 0.587074995 | 1 |
| attP40 Control 25°C ZT12 - Naam RNAi 25°C ZT18 | 1.020932184 | 1 |
| attP40 Control 25°C ZT12 - Naam RNAi 25°C ZT6 | 0.937922195 | 1 |
| attP40 Control 25°C ZT12 - Naam RNAi 30°C ZT0 | -1.335111304 | 1 |
| attP40 Control 25°C ZT12 - Naam RNAi 30°C ZT12 | -1.605720002 | 1 |
| attP40 Control 25°C ZT12 - Naam RNAi 30°C ZT18 | -0.1315677 | 1 |
| attP40 Control 25°C ZT12 - Naam RNAi 30°C ZT6 | -1.190923562 | 1 |
| attP40 Control 25°C ZT18 - attP40 Control 25°C ZT6 | 0.928137612 | 1 |
| attP40 Control 25°C ZT18 - attP40 Control 30°C ZT0 | -5.040647495 | 6.00E-05 |
| attP40 Control 25°C ZT18 - attP40 Control 30°C ZT12 | -6.025556039 | 2.82E-07 |
| attP40 Control 25°C ZT18 - attP40 Control 30°C ZT18 | -4.801958958 | 0.000189873 |
| attP40 Control 25°C ZT18 - attP40 Control 30°C ZT6 | -5.233004795 | 2.30E-05 |
| attP40 Control 25°C ZT18 - Naam RNAi 25°C ZT0 | 0.17507415 | 1 |
| attP40 Control 25°C ZT18 - Naam RNAi 25°C ZT12 | -1.181138979 | 1 |
| attP40 Control 25°C ZT18 - Naam RNAi 25°C ZT18 | -0.72446517 | 1 |
| attP40 Control 25°C ZT18 - Naam RNAi 25°C ZT6 | -0.830291779 | 1 |
| attP40 Control 25°C ZT18 - Naam RNAi 30°C ZT0 | -3.117759917 | 0.14831311 |

| | | |
|---|---|---|
| attP40 Control 25°C ZT18 - Naam RNAi 30°C ZT12 | -3.373933977 | 0.065544375 |
| attP40 Control 25°C ZT18 - Naam RNAi 30°C ZT18 | -1.899781674 | 1 |
| attP40 Control 25°C ZT18 - Naam RNAi 30°C ZT6 | -2.959137536 | 0.237141772 |
| attP40 Control 25°C ZT6 - attP40 Control 30°C ZT0 | -5.976361866 | 3.75E-07 |
| attP40 Control 25°C ZT6 - attP40 Control 30°C ZT12 | -6.953693651 | 7.96E-10 |
| attP40 Control 25°C ZT6 - attP40 Control 30°C ZT18 | -5.73009657 | 1.54E-06 |
| attP40 Control 25°C ZT6 - attP40 Control 30°C ZT6 | -6.161142407 | 1.26E-07 |
| attP40 Control 25°C ZT6 - Naam RNAi 25°C ZT0 | -0.753063461 | 1 |
| attP40 Control 25°C ZT6 - Naam RNAi 25°C ZT12 | -2.109276591 | 1 |
| attP40 Control 25°C ZT6 - Naam RNAi 25°C ZT18 | -1.640626311 | 1 |
| attP40 Control 25°C ZT6 - Naam RNAi 25°C ZT6 | -1.758429391 | 1 |
| attP40 Control 25°C ZT6 - Naam RNAi 30°C ZT0 | -4.053474288 | 0.005133222 |
| attP40 Control 25°C ZT6 - Naam RNAi 30°C ZT12 | -4.302071588 | 0.001849242 |
| attP40 Control 25°C ZT6 - Naam RNAi 30°C ZT18 | -2.827919286 | 0.344452774 |
| attP40 Control 25°C ZT6 - Naam RNAi 30°C ZT6 | -3.887275148 | 0.009760567 |
| attP40 Control 30°C ZT0 - attP40 Control 30°C ZT12 | -1.034097573 | 1 |
| attP40 Control 30°C ZT0 - attP40 Control 30°C ZT18 | 0.199488222 | 1 |
| attP40 Control 30°C ZT0 - attP40 Control 30°C ZT6 | -0.235076416 | 1 |
| attP40 Control 30°C ZT0 - Naam RNAi 25°C ZT0 | 5.217150846 | 2.46E-05 |
| attP40 Control 30°C ZT0 - Naam RNAi 25°C ZT12 | 3.849866405 | 0.01122527 |
| attP40 Control 30°C ZT0 - Naam RNAi 25°C ZT18 | 4.24433294 | 0.002336131 |
| attP40 Control 30°C ZT0 - Naam RNAi 25°C ZT6 | 4.203577711 | 0.002761306 |
| attP40 Control 30°C ZT0 - Naam RNAi 30°C ZT0 | 1.938845424 | 1 |
| attP40 Control 30°C ZT0 - Naam RNAi 30°C ZT12 | 1.639170743 | 1 |
| attP40 Control 30°C ZT0 - Naam RNAi 30°C ZT18 | 3.125357142 | 0.146403742 |
| attP40 Control 30°C ZT0 - Naam RNAi 30°C ZT6 | 2.057353333 | 1 |
| attP40 Control 30°C ZT12 - attP40 Control 30°C ZT18 | 1.223597081 | 1 |
| attP40 Control 30°C ZT12 - attP40 Control 30°C ZT6 | 0.792551244 | 1 |
| attP40 Control 30°C ZT12 - Naam RNAi 25°C ZT0 | 6.200630189 | 9.98E-08 |
| attP40 Control 30°C ZT12 - Naam RNAi 25°C ZT12 | 4.84441706 | 0.000155726 |
| attP40 Control 30°C ZT12 - Naam RNAi 25°C ZT18 | 5.223338502 | 2.40E-05 |
| attP40 Control 30°C ZT12 - Naam RNAi 25°C ZT6 | 5.19526426 | 2.73E-05 |
| attP40 Control 30°C ZT12 - Naam RNAi 30°C ZT0 | 2.95698515 | 0.237141772 |
| attP40 Control 30°C ZT12 - Naam RNAi 30°C ZT12 | 2.651622063 | 0.553832782 |
| attP40 Control 30°C ZT12 - Naam RNAi 30°C ZT18 | 4.125774365 | 0.003819285 |
| attP40 Control 30°C ZT12 - Naam RNAi 30°C ZT6 | 3.066418503 | 0.171552825 |
| attP40 Control 30°C ZT18 - attP40 Control 30°C ZT6 | -0.431045837 | 1 |
| attP40 Control 30°C ZT18 - Naam RNAi 25°C ZT0 | 4.977033108 | 8.21E-05 |
| attP40 Control 30°C ZT18 - Naam RNAi 25°C ZT12 | 3.620819979 | 0.027215028 |
| attP40 Control 30°C ZT18 - Naam RNAi 25°C ZT18 | 4.015530431 | 0.00588887 |
| attP40 Control 30°C ZT18 - Naam RNAi 25°C ZT6 | 3.971667179 | 0.006987559 |
| attP40 Control 30°C ZT18 - Naam RNAi 30°C ZT0 | 1.723399356 | 1 |
| attP40 Control 30°C ZT18 - Naam RNAi 30°C ZT12 | 1.428024981 | 1 |
| attP40 Control 30°C ZT18 - Naam RNAi 30°C ZT18 | 2.902177284 | 0.276799984 |
| attP40 Control 30°C ZT18 - Naam RNAi 30°C ZT6 | 1.842821422 | 1 |
| attP40 Control 30°C ZT6 - Naam RNAi 25°C ZT0 | 5.408078946 | 9.12E-06 |
| attP40 Control 30°C ZT6 - Naam RNAi 25°C ZT12 | 4.051865816 | 0.005133222 |
| attP40 Control 30°C ZT6 - Naam RNAi 25°C ZT18 | 4.441014154 | 0.001011 |
| attP40 Control 30°C ZT6 - Naam RNAi 25°C ZT6 | 4.402713016 | 0.001190878 |
| attP40 Control 30°C ZT6 - Naam RNAi 30°C ZT0 | 2.157963993 | 1 |
| attP40 Control 30°C ZT6 - Naam RNAi 30°C ZT12 | 1.859070819 | 1 |
| attP40 Control 30°C ZT6 - Naam RNAi 30°C ZT18 | 3.333223121 | 0.0749079 |
| attP40 Control 30°C ZT6 - Naam RNAi 30°C ZT6 | 2.273867259 | 1 |
| Naam RNAi 25°C ZT0 - Naam RNAi 25°C ZT12 | -1.356213129 | 1 |
| Naam RNAi 25°C ZT0 - Naam RNAi 25°C ZT18 | -0.897280204 | 1 |
| Naam RNAi 25°C ZT0 - Naam RNAi 25°C ZT6 | -1.00536593 | 1 |
| Naam RNAi 25°C ZT0 - Naam RNAi 30°C ZT0 | -3.294263268 | 0.08494426 |
| Naam RNAi 25°C ZT0 - Naam RNAi 30°C ZT12 | -3.549008127 | 0.035296203 |
| Naam RNAi 25°C ZT0 - Naam RNAi 30°C ZT18 | -2.074855825 | 1 |
| Naam RNAi 25°C ZT0 - Naam RNAi 30°C ZT6 | -3.134211687 | 0.143877544 |
| Naam RNAi 25°C ZT12 - Naam RNAi 25°C ZT18 | 0.441432668 | 1 |
| Naam RNAi 25°C ZT12 - Naam RNAi 25°C ZT6 | 0.3508472 | 1 |
| Naam RNAi 25°C ZT12 - Naam RNAi 30°C ZT0 | -1.926978828 | 1 |
| Naam RNAi 25°C ZT12 - Naam RNAi 30°C ZT12 | -2.192794998 | 1 |
| Naam RNAi 25°C ZT12 - Naam RNAi 30°C ZT18 | -0.718642695 | 1 |
| Naam RNAi 25°C ZT12 - Naam RNAi 30°C ZT6 | -1.777998557 | 1 |
| Naam RNAi 25°C ZT18 - Naam RNAi 25°C ZT6 | -0.095112718 | 1 |
| Naam RNAi 25°C ZT18 - Naam RNAi 30°C ZT0 | -2.346656652 | 1 |
| Naam RNAi 25°C ZT18 - Naam RNAi 30°C ZT12 | -2.605932351 | 0.623531924 |
| Naam RNAi 25°C ZT18 - Naam RNAi 30°C ZT18 | -1.150802165 | 1 |
| Naam RNAi 25°C ZT18 - Naam RNAi 30°C ZT6 | -2.196488347 | 1 |
| Naam RNAi 25°C ZT6 - Naam RNAi 30°C ZT0 | -2.280690134 | 1 |
| Naam RNAi 25°C ZT6 - Naam RNAi 30°C ZT12 | -2.543642197 | 0.734479601 |
| Naam RNAi 25°C ZT6 - Naam RNAi 30°C ZT18 | -1.069489895 | 1 |
| Naam RNAi 25°C ZT6 - Naam RNAi 30°C ZT6 | -2.128845757 | 1 |
| Naam RNAi 30°C ZT0 - Naam RNAi 30°C ZT12 | -0.283716834 | 1 |
| Naam RNAi 30°C ZT0 - Naam RNAi 30°C ZT18 | 1.202469564 | 1 |

| | | |
|---|---|---|
| Naam RNAi 30°C ZT0 - Naam RNAi 30°C ZT6 | 0.134465755 | 1 |
| Naam RNAi 30°C ZT12 - Naam RNAi 30°C ZT18 | 1.474152302 | 1 |
| Naam RNAi 30°C ZT12 - Naam RNAi 30°C ZT6 | 0.41479644 | 1 |
| Naam RNAi 30°C ZT18 - Naam RNAi 30°C ZT6 | -1.059355862 | 1 |